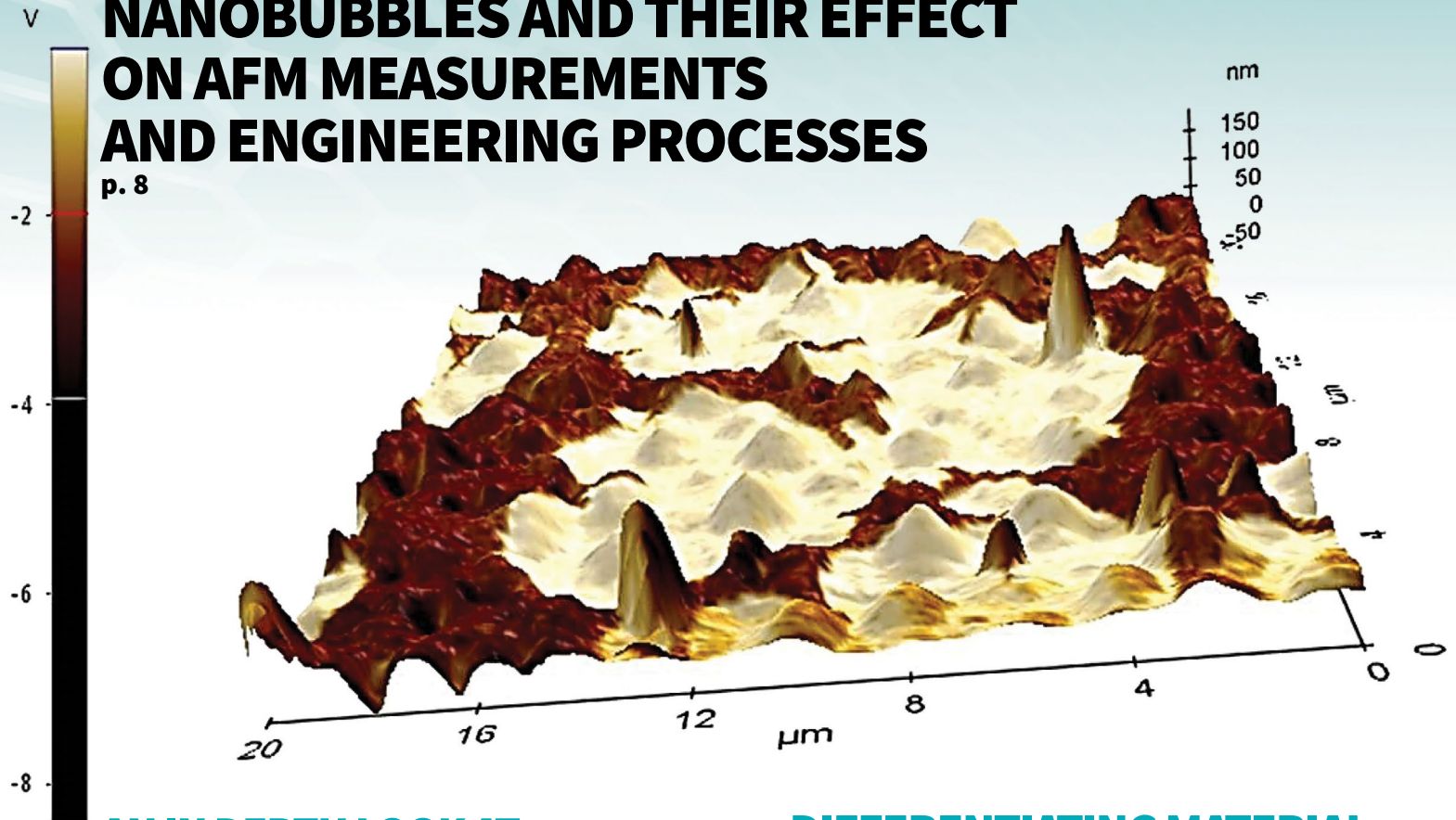## INSIGHTS INTO SUBMICRON-SCALES - NANOBUBBLES AND THEIR EFFECT ON AFM MEASUREMENTS AND ENGINEERING PROCESSES
p. 8

TABLE
OF CONTENTS

NanoScientific Vol 14 Fall 2018

p. 8

p. 20

p. 24

NANOscientific is published quarterly to showcase advancements in the field of nanoscience and technology across a wide range of multidisciplinary areas of research. The publication is offered free to anyone who works in the field of nanotechnology, nanoscience, microscopy and other related fields of study and manufacturing.

We would enjoy hearing from you, our readers. Send your research or story ideas to **debbiewest@ nanoscientific.org**

To view all of our articles, please visit our web site at **www.nanoscientific.org.**

INSET PHOTO ON COVER:

This image shows a 3D overlay of a frictional response map and topographical data acquired using Park AFM's Lateral Force Microscopy (LFM) from a polymer coated on a glass sample.

Homogeneously distributed circular features within the sample can be seen from the topography, and the two materials are not easily distinguishable.

However, two components with dramatically different frictional properties were clearly observed from the LFM image. Brighter areas show a relatively larger friction coefficient response and darker areas a smaller friction coefficient response.

This result clearly showcases that LFM is ideal to analyze samples which consist of heterogeneous compositions with different frictional coefficients.

Park SYSTEMS

NanoScientific Symposium on SPM at SUNY Polytechnic – Key Speakers & Topics

Dr. Rigoberto Advincula "Functional Graphene Oxide (GO) Templated Patterning and Anti-Microbial Properties" Professor at the Dept. of Macromolecular Science and Engineering, Case Western Reserve University, Director of PETRO Case, a polymers for oil-gas consortium and editor-in-chief of MRS Communications.

Dr. Alain Diebold SUNY Polytechnic Institute, Interim Dean of the College of Nanoscale Science; Empire Innovation Professor of Nanoscale Science; Executive Director, Center for Nanoscale Metrology " Measurement Challenges arising from New Semiconductor Materials and Structures for Integrated Circuits"

Dr. Gwo Ching-Wang Rensselaer Polytechnic Institute (RPI), Travelstead Institute Chair, Physics, Applied Physics & Astronomy "Ultrathin layered materials studied by AFM and MFM"

Phil Kaszuba Global Foundries Senior Member of Technical Staff and lead engineer in their Scanning Probe Microscopy (SPM) laboratory "Meeting the Challenges in Analyzing State-of-the-art Semiconductor Devices Using Scanning Probe Microscopy"

Dr. Yiping Zhao Professor, Department of Physics and Astronomy, Director, Nanoscale Science and Engineering Center, The University of Georgia "When glancing angle deposition meets with colloidal lithography … "

Dr. Ye Tao Rowland Institute at Harvard "Learning in Fundamental Atomistic Processes Using Suspended Silicon Nanowires"

Dr. John A Marohn, Professor& Director of Undergraduate Studies, Department of Chemistry and Chemical Biology Member, Field of Materials Science & Engineering, Cornell University "Advances in Electric Force Microscopy: (1) Sub-cycle Changes in Photocapacitance in Organic Photovoltaics, (2) Anomalous Light-induced Conductivity in Lead-Halide Perovskites, and (3) a Unified Lagrangian-Mechanics Theory of Scanning-Probe Electrical Measurements"

Dr. Jiahua Zhu PhD, University of Akron, Associate Professor, Department of Chemical and Biomolecular Engineering "Quantitative Thermal Conductivity Analysis with Scanning Thermal Microscopy"

Dr. Nancy A. Burnham, Associate Prof of Physics & Associate Prof of Biomedical Engineering, Worcester Polytechnic Institute "The Complex Polymers Beneath Your Feet"

MESSAGE
FROM EDITOR

Greetings!

Nanotechnology's impact on the world of science and engineering has had an enormous influence on future technologies. With the global technology market expected to exceed $125 Billion by 2024, nanosized particles are changing virtually every sector of our society.

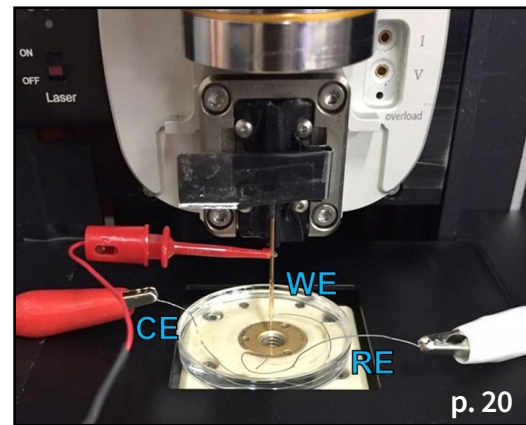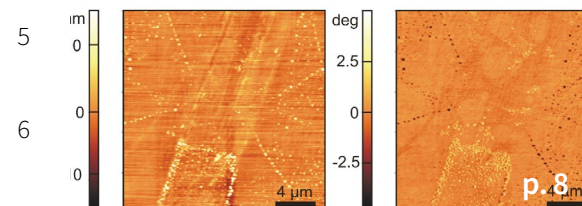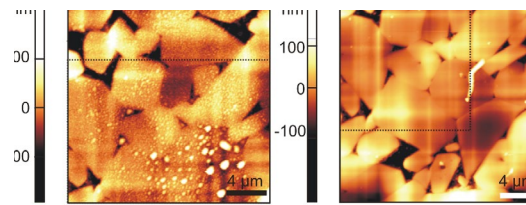In this issue of NanoScientific, we have two articles from presenters at the NanoScientific Symposium in Europe, "Insights into Submicron-Scales - Nanobubbles and Their Effect on AFM Measurements and Engineering Processes" by Lisa Ditscherlein, Technical University Freiberg and an interview with Tobias Cramer Asst. Professor, Department of Physics and Astronomy, Bologna, Italy with "An In Depth Look at Implantable Organic Nano Electronics".

We also have a feature interview with Dr. Elliott Bloom from Stanford about the search for dark matter and other wonders of the universe for the last ten years using the Large Area Telescope on the Fermi Gamma-ray space observatory at Stanford.

We have two application notes on Simultaneous Topographical and Electrochemical Mapping using Scanning Ion Conductance Microscopy – Scanning Electrochemical Microscopy (SICM-SECM) and Differentiating Material Compositions using Lateral Force Microscopy.

Scanning Probe Microscopy (SPM) advances the researchers ability to see and analyze nanoparticles in new ways and in more depth. The advancements in nanometrology run parallel with the advances in nanoscience and nanotechnology. NanoScientific is proud to present NanoScientific Symposiums on SPM world-wide. This year we are sponsoring three symposiums in Korea, the United States and Europe.

Aug. 22-23, 2018 NanoScientific Symposium on SPM at Korea Advanced Nano Fab Center in Korea

Register here: www.parksystems.com/ index.php/events/nanoscientific-korea

Sept.19-20, 2018 NanoScientific Symposium on SPM at SUNY Polytechnic Institute in Albany New York

Register here: www.parksystems.com/ spm2018

Oct. 10-12, 2018 NanoScientific Symposium on SPM at Technical University Freiberg, Germany

Register here: www.parksystems.com/ nsfe2018

We hope you can join us at one of these or future upcoming NanoScientific Symposiums and as always, send us your feedback and story ideas.

Keibock Lee
Editor-in-Chief

The NanoScientific Symposium on SPM will be held Sept. 19-20 at the Park Nanoscience Center at SUNY Poly's Albany NanoTech Complex, a fully-integrated research, development, prototyping, and educational facility and home to the College of Nanoscale Sciences and the College of Nanoscale Engineering and Technology Innovation.

Park Systems, Sponsor of NanoScientific Symposium on SPM at SUNY Polytechnic is offering Complimentary Registration thru Sept. 10

2018 NanoScientific Symposium
Scanning Probe Microscopy

September 19-20, 2018 • SUNY Polytechnic Institute, Albany, NY

Park SYSTEMS

NanoScientific Symposium Sponsor Park Systems is offering Complimentary Registration Until Sept. 10

Register Today at https://parksystems.com/spm2018

Park Systems and NanoScientific Publications are proud to announce the

2018 NANOSCIENTIFIC SYMPOSIUM ON SCANNING PROBE MICROSCOPY (SPM)

A new venue for nanoscience researchers, scientists, and engineers to learn about the latest studies being formed using SPM. Keynote speakers from both academia and industry will be on hand to talk about the current cutting-edge work being performed in their laboratories and discuss the headway they have made with SPM in some of the hottest fields and topics in nanoscience today.

DO NOT MISS YOUR CHANCE TO JOIN THIS GREAT OPPORTUNITY TO LEARN AND NETWORK WITH SOME OF THE BEST AND BRIGHTEST IN MATERIALS CHARACTERIZATION!

The first day, Wednesday, September 19, will be composed of keynote speakers and presenters on a variety of topics including the following:

- 2D and other nanomaterials
- Polymers and composites
- Electronics, magnetics, and photonics
- Sustainable energy applications
- Semiconductor and MEMS process and fabrication
- Analytical chemistry
- Biology, biomedicine, and other life sciences

The evening networking event will include cocktails and hors d'oeuvres.

The second day, Thursday, September 20, will focus on hands-on programming:

A theory and practical class on AFM with access to live systems at the Park Nanoscience Center at SUNY Polytechnic Institute.

"As SUNY Polytechnic Institute provides cutting-edge educational and research and development opportunities, it is exciting that Park Systems established operations at our Albany campus," said Dr. Alain Diebold, SUNY Poly Interim Dean of the College of Nanoscale Sciences; Empire Innovation Professor of Nanoscale Science; and Executive Director, Center for Nanoscale Metrology. "Our scientists and engineers look forward to working closely with Park Systems to enhance next-generation technologies that will lead to improved metrology capabilities for researchers and members of industry around the world."

REGISTER ONLINE TODAY AT:
http://parksystems.com/spm2018

2018 NanoScientific Forum Europe NSFE 2018
Scanning Probe Microscopy (SPM)

10-12 October, 2018
TU Bergakademie Freiberg, Germany

Sponsored by Park Systems, TU Bergakademie Freiberg & NANOscientific Magazine

IMPORTANT DEADLINES

Registration for the conference is open until September 30

Abstract / image submission is open until June 30

REGISTER TODAY FOR THE NANOSCIENTIFIC SYMPOSIUM ON SCANNING PROBE MICROSCOPY (SPM) IN EUROPE AT THE TECHNICAL UNIVERSITY FREIBERG, GERMANY OCTOBER 10-12, 2018

TU Bergakademie Freiberg (TU Freiberg), Institute of Mechanical Process Engineering and Mineral Processing host of the 1st NanoScientific Forum Europe 2018 (NSFE 2018) will give a special session during the scientific program on nanobubbles, which is a part of the flagship project on nanobubbles in engineering processes like melt filtration (CRC 920, a flagship project of TU Freiberg) and flotation (SPP2045, TU Freiberg and Helmholtz Institute Freiberg for Resource Technology).

This 2 Day Event will include lectures by renowned AFM researchers, Instrument workshops on Park Systems AFMs, including basic and advanced measuring techniques as well as tips and tricks, how to obtain stunning AFM data.

Wednesday Evening: Fusing Science & People - Conference Gala Dinner

Thursday Evening: Discovering Natural Treasures - terra mineralia Tour & Party

CONFERENCE TOPICS

Application:

- Geoscience and sustainable energy applications
- Polymers and composites
- Nanoelectronics, photonic and photovoltaic applications
- Nanomaterials and Life Science
- Special Session nanobubbles

Method:

- Nanomechanical and Electrical Characterization
- Characterization Techniques in Aqueous Solution
- Advanced Imaging

NANOScientific Publications announces the **2018 NANOSCIENTIFIC SYMPOSIUMS ON SCANNING PROBE MICROSCOPY (SPM)** new venues for nanoscience researchers, scientists, and engineers to learn about the latest studies being formed using SPM. Keynote speakers from both academia and industry will talk about cutting-edge work being performed in their laboratories and the hottest topics in nanoscience today - sponsored by NanoScientific and Park Systems. Poster and Oral Presentation Opportunities, submit your abstract today.

NanoScientific Symposium on SPM in Europe – Oct. 10-12, 2018 at Frieberg University **www.parksystems.com/nsfe2018**

NanoScientific Symposium on SPM in US – Sept 19-20 at SUNY Polytechnic Institute **www.parksystems.com/2018spm**

REGISTER ONLINE TODAY AT:
http://parksystems.com/nsfe2018

INSIGHTS INTO SUBMICRON-SCALES

NANOBUBBLES AND THEIR EFFECT ON AFM MEASUREMENTS AND ENGINEERING PROCESSES

Lisa Ditscherlein,
Scientific Researcher (PhD) at MVTAT, TU Bergakademie Freiberg, Mechanical Process Engineering and Material Processing, Specialization Particle Technology

Since the invention of devices like the surface force apparatus in 1969[1]and the atomic force microscope(AFM) in 1986[2], surface forces have been studied extensively by many scientists[3] as properties of the interfacial region are of great interest for a variety of engineering processes. Interactions between two surfaces are often quantified by classical DLVO-theory, but this theory fails if two hydrophobic surfaces approach each other in an aqueous solution. Other non-DLVO forces come into play that are of different nature and enhance attractive interactions[4]. The origin of such "hydrophobic forces" is still unknown and it is still not clear if it should be considered as a solvation force or some kind of long-ranged electrostatic or van der Waals interaction. Currently "hydrophobic forces" are considered to consist of two parts: a short-ranged true hydrophobic and a long-ranged force,induced by capillary interactions. In 1994, Parker et al. were the first who proclaimed that small bridging bubbles are responsible for the long-ranged, large interaction between hydrophobic surfaces [5]. They observed steps in force-distance curves and interpreted them as coalescing nanobubbles.Some years later, in 2000, Lou et al. [6] and Ishida et al. [7] developed independently a reproducible method to generate nanobubbles on surfaces. Since then, many investigations were done on nanobubble generation[8], stability[9], size and geometry [10-13], detection methods[14], sample roughness[15] and also their impact on engineering processes and other applications.

In most publications, nanobubbles are generated by the so-called solvent exchange method: Here, a liquid (in most cases ethanol) with high gas solubility is replaced by a liquid with lower solubility. This leads to a local gas oversaturation and the nucleation of the bubbles [16]. Another technique is based on the same principle of gas oversaturation: sample or liquid are heated and a local temperature gradient on the surface leads to the creation of the bubbles [17]. The existence of nanobubbles has been debated for a long time, because they should dissolve in microseconds [18] but were stable for hours and even days [19]. Brenner and Lohse[20] introduced an interesting model,where the stability of the bubbles is ensured by a dynamic equilibrium between flux of gas in and out of the nanobubble,which has been further improved by Yasui et al. [21]. A dense gas layer on the surface provides enough gas for the influx in the bubble. Today it is believed that the long-time stability of nanobubbles is caused by a combination of supersaturation and contact line pinning [22, 23] which accompanies the dynamic equilibrium theory. What has been seen by Zhang and co-workers is a shrinkage of the nanobubble contact angle instead of lateral size[24].The bubble stays pinned on the three phase contact line, the Laplace pressure diverges to zero and no large inner pressure or concentration gradient between nanobubble and surrounding environment occurs. Pinning takes place due to chemical and morphological inhomogenities, even at very smooth and clean surfaces.

$$d = 2\sqrt{2rh - h^2}$$
$$\theta = 180° - 2\arctan(2h/d)$$

range of nanobubble size described in literature:
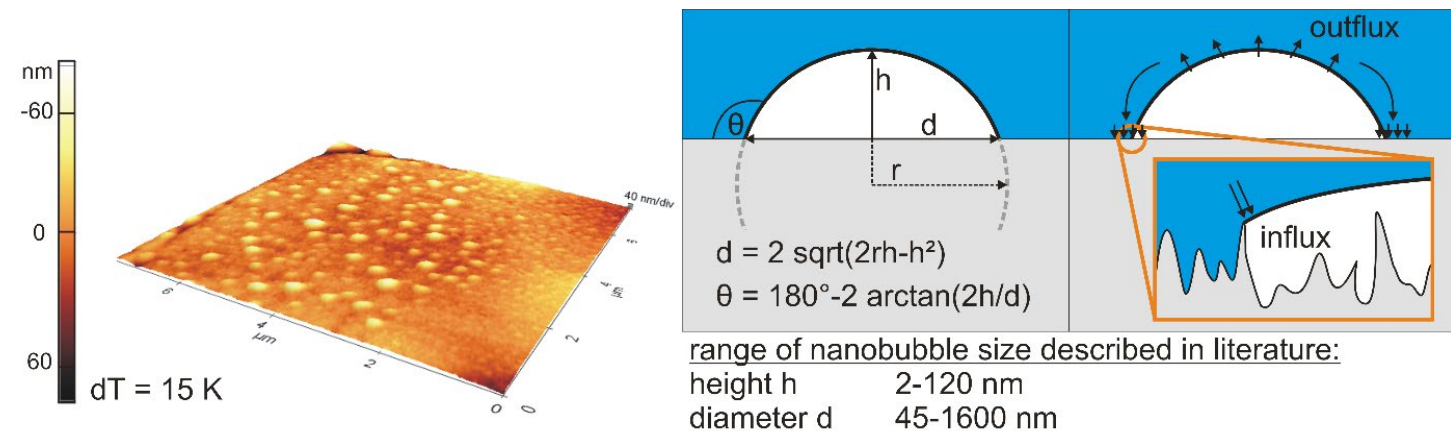height h   2-120 nm
diameter d   45-1600 nm

Figure 1: 3D topographical scan (isotropic axes) of a hydrophobic rough surface covered with small cap-shaped nanobubbles generated via gas oversaturation (left), geometrical parameters (middle) and scheme of stability theory (right)

With phase contrast imaging it is possible to distinguish between nanobubbles and contaminations.

In the past years, most nanobubble investigations were done using atomic force microscopy because it is a powerful tool to analyse microscopic surfaces. In principle, one can use AFM to scan the surface for bubbles directly via different scanning modes[25, 26] or indirectly via force spectroscopy[27]. Contact mode is unsuitable due to the lateral force applied to the nanobubbles which lets them coalesce or even detach from the surface. This mode has only been used to prove the soft character of the cap-shaped domes [27]. Commonly, intermittent/Tapping® mode is applied to detect the bubbles since lateral forces are minimized as a consequence of cantilever oscillation. Amplitude ratios (set point amplitude to free amplitude) should lie above 0.7 as otherwise deformation of the bubbles becomes strong [28, 29] and distorts the result. Often, phase contrast imaging is done simultaneously to facilitate the distinction between bubble and surface. A more seldom-used method is frequency modulation/true non-contact mode. Here, the cantilever oscillates at its resonant frequency close to the nanobubble-covered sample with a small amplitude without touching it. With this mode, deformation of nanobubbles is minimized. In recent years, the PeakForce® mode has been used for nanobubble detection as well. This mode works at frequencies below resonance and tracks the maximum force load on the tip in real time—which is advantageous compared to tapping mode, where it is difficult to quantify this force. An influencing factor is the chosen imaging force: the larger the force, the higher the deformation of the bubbles. In order to detect nanobubbles it is obvious that a soft and sharp cantilever is needed due to the soft matter character of the bubbles. Normally, cantilevers with spring constants between 0.2 and 4.8 N/m are used. It is to say that, besides AFM mode, the cantilever tip influences the scanning results [30]so that a recalculation of the geometrical size is necessary, if possible. Although the AFM provides three-dimensional information there are some drawbacks: a perturbation of the nanobubbles by the tip is inevitable. Another problem is the inability of the AFM to distinguish between gaseous domains and contamination: it is important to work under clean conditions, e.g. using only glass syringes and clean cantilevers [31].Therefore, alternative observation techniques are utilized like rapid cryofixation[32], infrared spectroscopy to determine the presence of nanobubbles[33], interference-enhanced reflection microscopy [34] to study bubble growth, attenuated total internal reflection microscopy in combination with other spectroscopic methods that investigate the formation of nanobubbles [35], or confocal microscopy to name but a few.
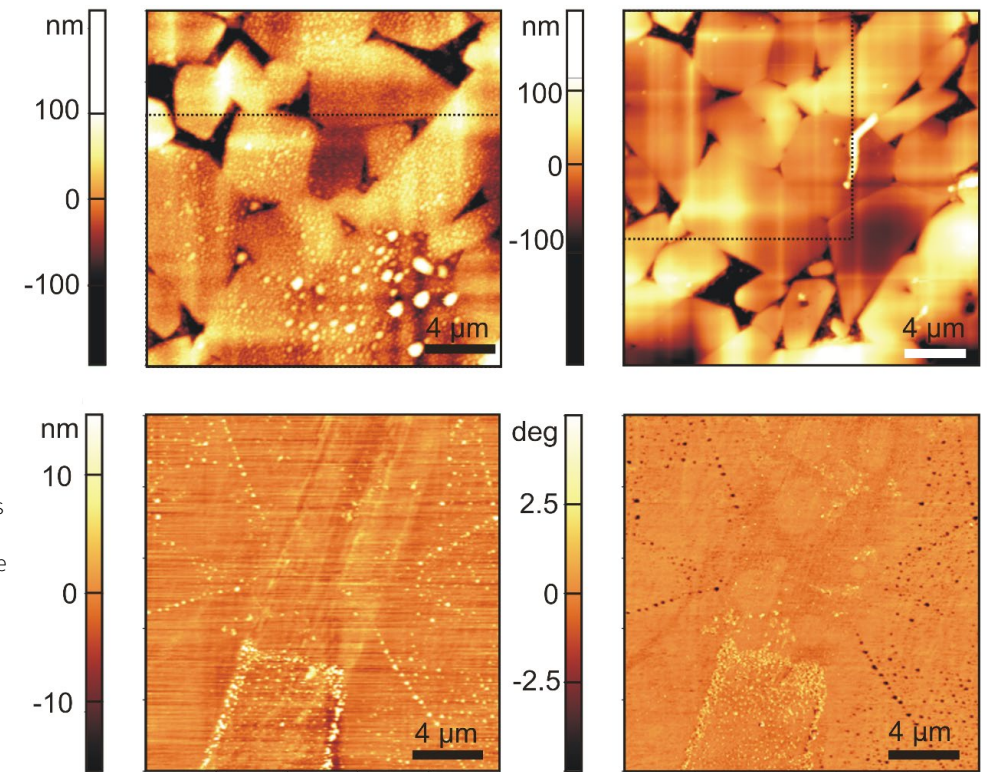
Figure 2: 2D topographical scan (top) of a rough hydrophobic surface in water with nanobubbles (left) and after drying (right) and 2D topographical scan and phase contrast image of a hydrophobic smooth surface.
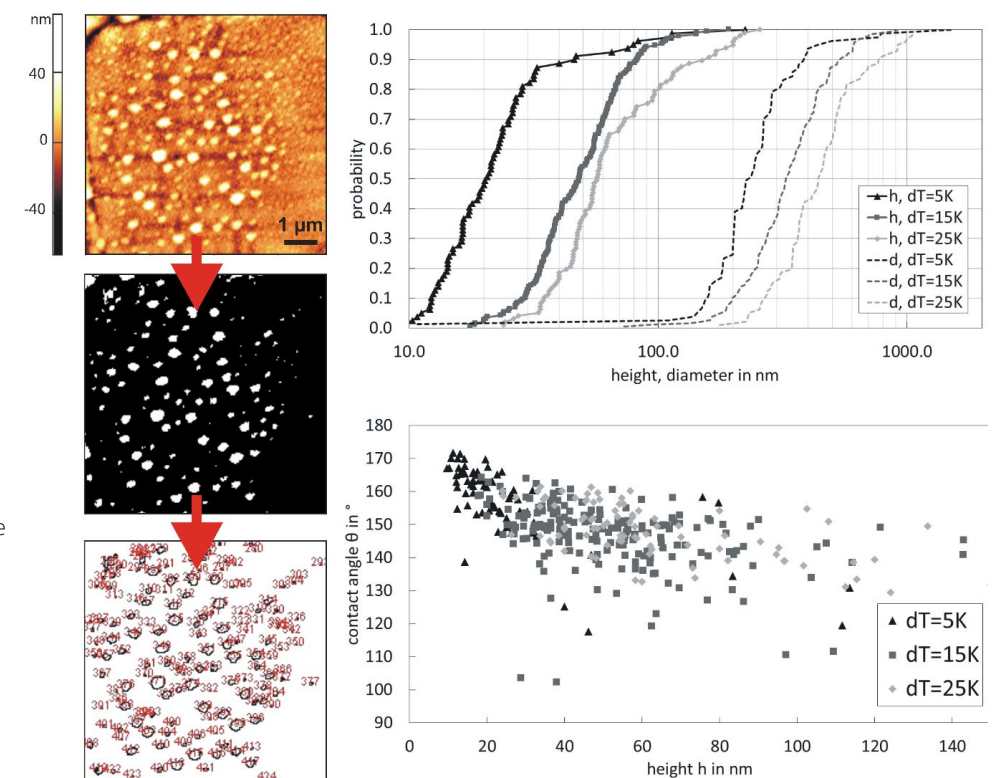
Figure 3: Evaluation of nanobubbles on a rough hydrophobic surface via ImageJ by binarisation (a certain threshold has to be chosen), geometrical size distributions of nanobubbles and dependency of contact angle on height for different temperature gradients.
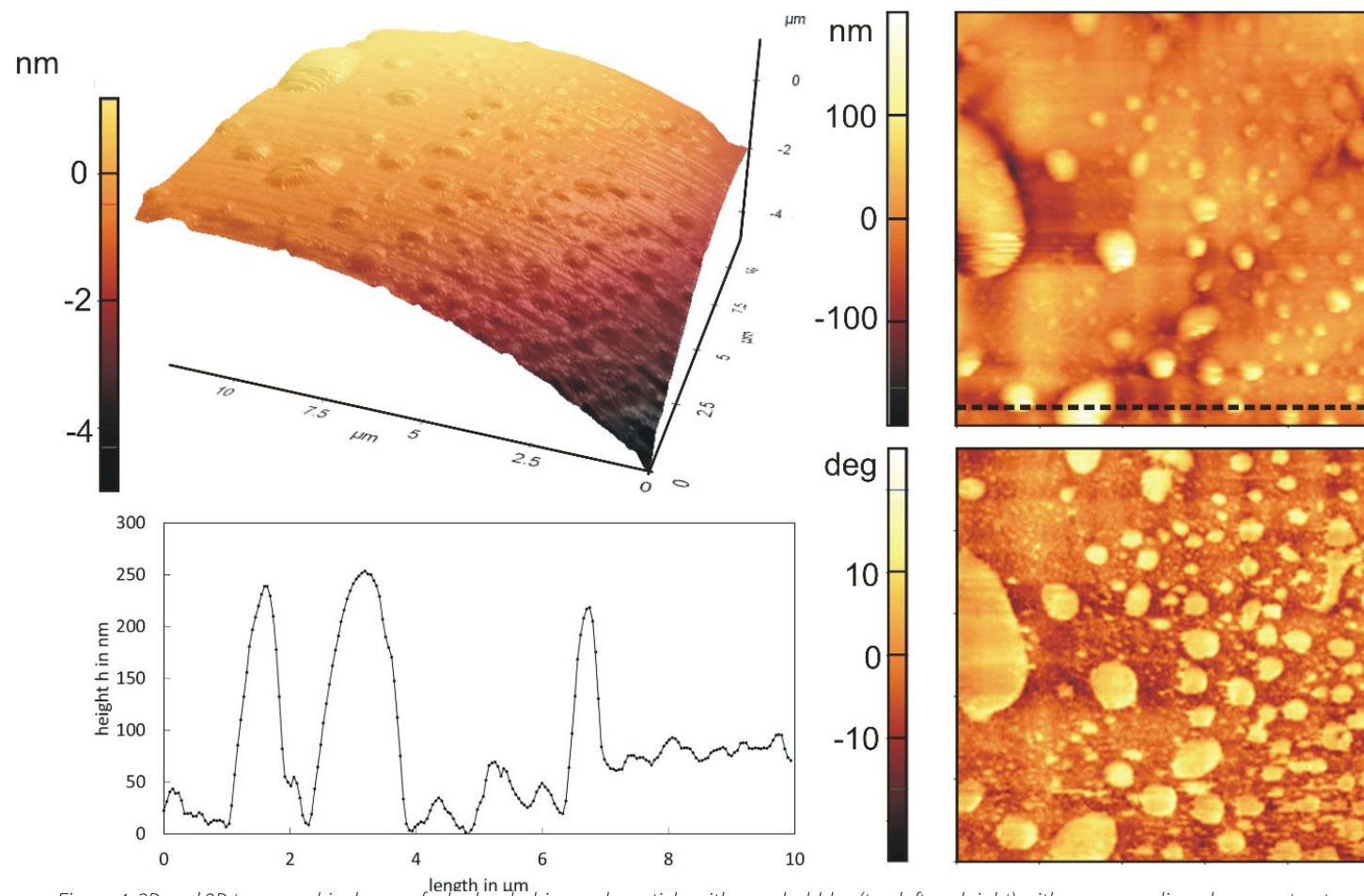
Figure 4: 3D and 2D topographical scan of a hydrophobic rough particle with nanobubbles (top left and right) with corresponding phase contrast image (bottom right) and line profile (bottom left).

Figure 5: agglomerate size (left) and particle-particle interaction dependency on wetting properties. The formation of nanobubbles leads to larger adhesive forces and therefore larger agglomerates

Interestingly, nearly all examined surfaces like silanized Si-wafers, mica, HOPG or PS are relatively smooth with rms <5 nm. Such samples are quite interesting in order to acquire fundamental understanding about the formation and stability of nanobubbles as well as the impact of the chosen measurement device on the results. In nearly all real world engineering processes one has to deal with technically rough (rms > 100 nm) and often inhomogeneous surfaces like crushed particles, sintered or abraded surfaces. Measurement on rough surfaces is more complicated, since peaks and valleys influence results if parameters are improperly set and it is often more time-consuming. For such surfaces there is a need for statistically valid results because of the highly variable interaction area that changes from point to point. This can only be accomplished by a comprehensive sampling and a high number of measurements. Consequently, for force distance spectroscopy hundreds or thousands of curves and an evaluation routine becomes necessary. Previous works on rough surfaces show the impact of wettability and roughness on nanobubble count, stability and therefore adhesive interactions [36-38]: whilst the probability of capillary interactions is low

on hydrophilic surfaces (θ = 80°), it is more than doubled on hydrophobic samples (θ = 104°). This leads to much stronger adhesion between the two surfaces. Contrary to results for hydrophilic systems, adhesion is increased with higher roughness. The explanation for this behaviour is a larger amount of bubbles nested in a stable position inside the pores and asperities. On the other hand, access for the second interacting surface to the nanobubble has to be ensured as otherwise no capillary bridge is formed. Another, very interesting aspect seen on slightly rough, but also on technical rough surfaces, is the increased stability of nanobubbles. Only small contact forces (below 5 nN) are necessary to move bubbles on smooth surfaces. In contrast, on rough surfaces they are only deformed but keep pinned to the asperities and pores. Contact forces tenfold stronger are needed to move them.

Engineering processes like flotation, agglomeration or filtration benefit from the microscopic findings about nanobubbles and can be optimized. For mineral flotation, an engineering process that separates hydrophobic from hydrophilic materials, the attachment between bubble and valuable

material is of great importance. Normally, good flotation performance is limited to particle sizes between 10 and 100 μm (minerals) or 50 to 600 μm (coal). Nanobubbles can increase the recovery of finer particles by improving film rupture [39, 40] and have been studied for coal, sheelite, chalcopyrite and quartz. Less frother is necessary because they stabilize the froth and the necessary amount of air is reduced [41]. A large quantity of submicron bubbles can be achieved by ultrasound or hydrodynamic cavitation [42]. Progress is made in the field of nanobubble-nanoparticle contact. Contrary to froth flotation, particle-bubble contact is not achieved by collision but by new nucleation of nanobubbles directly onto the nanoparticles [43]. Agglomeration, another engineering process, is also strongly influenced by the presence of the bubbles. Nanobubbles promote agglomeration between hydrophobic particles due to capillary interactions between them, a phenomenon that holds true for fine as well as coarse particles [44]. In [45], an enhancement of agglomeration can be seen in agglomeration size and particle-particle interactions. Furthermore, agglomerates that contain nanobubbles are more stable at higher shear rates[46]. In deep bed filtration experiments, an improvement of filtration
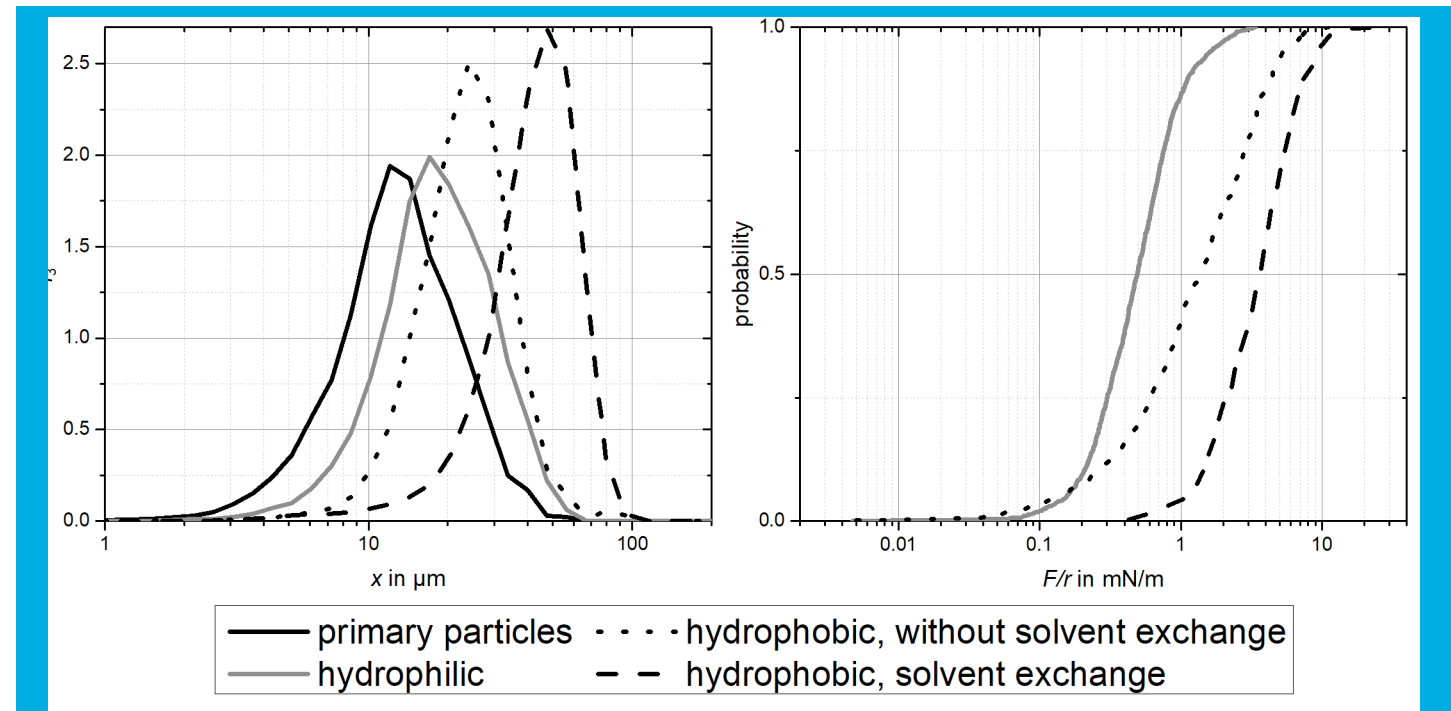
efficiency can be observed, too. Here, nanobubbles are sitting on poorly wetted foam filters and keep inclusion particles trapped [37]. The amount of nanobubbles determines the degree of efficiency. These results are not only interesting for conventional deep bed filtration processes but also for the purification of metal melts [47, 48].

There are many more promising fields for the application of nanobubbles like wastewater treatment [49], micro- and nanofluidics[50] or electrolysis [51]. The research topic "nanobubbles" provides interesting opportunities in the next few years. It remains exciting.

[1] D. Tabor and R. H. S. Winterton, "The direct measurement of normal and retarded van der Waals forces," Proceedings of the Royal Society of London. A. Mathematical and Physical Sciences, vol. 312, pp. 435-450, 1969.
[2] G. Binnig, C. F. Quate, and C. Gerber, "Atomic force microscope," Physical Review Letters, vol. 56, pp. 930-933, 1986.
[3] J. N. Israelachvili, Intermolecular and Surface Forces, 3 ed. Oxford: Elsevier LTD., 2011.
[4] H. K. Christenson and P. M. Claesson, "Direct measurements of the force between hydrophobic surfaces in water," Advances in Colloid and Interface Science, vol. 91, pp. 391-436, 2001.
[5] J. L. Parker, P. M. Claesson, and P. Attard, "Bubbles, cavities, and the long-ranged attraction between hydrophobic surfaces," Journal of Physical Chemistry®, vol. 98, pp. 8468-8480, 1994.
[6] S. T. Lou, Z. Q. Ouyang, Y. Zhang, X. J. Li, J. Hu, M. Q. Li, et al., "Nanobubbles on solid surface imaged by atomic force microscopy," Journal of Vacuum Science and Technology B: Microelectronics and Nanometer Structures, vol. 18, pp. 2573-2575, 2000.
[7] N. Ishida, T. Inoue, M. Miyahara, and K. Higashitani, "Nano bubbles on a hydrophobic surface in water observed by tapping-mode atomic force microscopy," Langmuir, vol. 16, pp. 6377-6380, 2000.
[8] M. A. J. Van Limbeek and J. R. T. Seddon, "Surface nanobubbles as a function of gas type," Langmuir, vol. 27, pp. 8694-8699, 2011.
[9] Y. Sun, G. Xie, Y. Peng, W. Xia, and J. Sha, "Stability theories of nanobubbles at solid-liquid interface: A review," Colloids and Surfaces A: Physicochemical and Engineering Aspects, vol. 495, pp. 176-186, 2016.
[10] R. P. Berkelaar, J. R. T. Seddon, H. J. W. Zandvliet, and D. Lohse, "Temperature dependence of surface nanobubbles," ChemPhysChem, vol. 13, pp. 2213-2217, 2012.
[11] B. Bhushan, Y. Pan, and S. Daniels, "AFM characterization of nanobubble formation and slip condition in oxygenated and

electrokinetically altered fluids," Journal of Colloid and Interface Science, vol. 392, pp. 105-116, 2013.
[12] B. M. Borkent, S. De Beer, F. Mugele, and D. Lohse, "On the shape of surface nanobubbles," Langmuir, vol. 26, pp. 260-268, 2010.
[13] D. Li and X. Zhao, "Micro and nano bubbles on polystyrene film/ water interface," Colloids and Surfaces A: Physicochemical and Engineering Aspects, vol. 459, pp. 128-135, 2014.
[14] D. Lohse and X. Zhang, "Surface nanobubbles and nanodroplets," Reviews of Modern Physics, vol. 87, 2015.
[15] J. Yang, J. Duan, D. Fornasiero, and J. Ralston, "Very small bubble formation at the solid-water interface," Journal of Physical Chemistry B, vol. 107, pp. 6139-6147, 2003.
[16] M. A. Hampton, B. C. Donose, and A. V. Nguyen, "Effect of alcohol-water exchange and surface scanning on nanobubbles and the attraction between hydrophobic surfaces," Journal of Colloid and Interface Science, vol. 325, pp. 267-274, 2008.
[17] C. Xu, S. Peng, G. G. Qiao, V. Gutowski, D. Lohse, and X. Zhang, "Nanobubble formation on a warmer substrate," Soft Matter, vol. 10, pp. 7857-7864, 2014.
[18] S. Ljunggren and J. C. Eriksson, "The lifetime of a colloid-sized gas bubble in water and the cause of the hydrophobic attraction," Colloids and Surfaces A: Physicochemical and Engineering Aspects, vol. 129-130, pp. 151-155, 1997.
[19] X. H. Zhang, A. Quinn, and W. A. Ducker, "Nanobubbles at the interface between water and a hydrophobic solid," Langmuir, vol. 24, pp. 4756-4764, 2008.
[20] M. P. Brenner and D. Lohse, "Dynamic equilibrium mechanism for surface nanobubble stabilization," Physical Review Letters, vol. 101, 2008.
[21] K. Yasui, T. Tuziuti, W. Kanematsu, and K. Kato, "Advanced dynamic-equilibrium model for a nanobubble and a micropancake on a hydrophobic or hydrophilic surface," Physical Review E - Statistical, Nonlinear, and Soft Matter Physics, vol. 91, 2015.
[22] Y. Liu and X. Zhang, "A unified mechanism for the stability of surface nanobubbles: Contact line pinning and supersaturation," Journal of Chemical Physics, vol. 141, 2014.
[23] D. Lohse and X. Zhang, "Pinning and gas oversaturation imply stable single surface nanobubbles," Physical Review E, vol. 91, p. 031003, 03/27/ 2015.
[24] X. Zhang, D. Y. C. Chan, D. Wang, and N. Maeda, "Stability of interfacial nanobubbles," Langmuir, vol. 29, pp. 1017-1023, 2013.
[25] W. Walczyk, P. M. Schön, and H. Schönherr, "The effect of PeakForce tapping mode AFM imaging on the apparent shape of surface nanobubbles," Journal of Physics Condensed Matter, vol. 25, 2013.
[26] C. W. Yang, Y. H. Lu, and I. S. Hwang, "Imaging surface nanobubbles at graphite-water interfaces with different atomic force microscopy modes," Journal of Physics Condensed Matter, vol. 25, 2013.
[27] L. Ditscherlein, J. Fritzsche, and U. A. Peuker, "Study of nanobubbles on hydrophilic and hydrophobic alumina surfaces," Colloids and Surfaces A: Physicochemical and Engineering Aspects, vol. 497, pp. 242-250, 2016.
[28] X. H. Zhang, N. Maeda, and V. S. J. Craig, "Physical properties of nanobubbles on hydrophobic surfaces in water and aqueous solutions," Langmuir, vol. 22, pp. 5025-5035, 2006.
[29] S. Yang, E. S. Kooij, B. Poelsema, D. Lohse, and H. J. W. Zandvliet, "Correlation between geometry and nanobubble distribution on HOPG surface," EPL, vol. 81, 2008.
[30] W. Walczyk and H. Schönherr, "Characterization of the interaction between AFM tips and surface nanobubbles," Langmuir, vol. 30, pp. 7112-7126, 2014.
[31] R. P. Berkelaar, E. Dietrich, G. A. M. Kip, E. S. Kooij, H. J. W. Zandvliet, and D. Lohse, "Exposing nanobubble-like objects to a degassed environment," Soft Matter, vol. 10, pp. 4947-4955, 2014.

[32] M. Switkes and J. W. Ruberti, "Rapid cryofixation/freeze fracture for the study of nanobubbles at solid-liquid interfaces," Applied Physics Letters, vol. 84, pp. 4759-4761, 2004.
[33] X. H. Zhang, A. Khan, and W. A. Ducker, "A nanoscale gas state," Physical Review Letters, vol. 98, 2007.
[34] S. Karpitschka, E. Dietrich, J. R. T. Seddon, H. J. W. Zandvliet, D. Lohse, and H. Riegler, "Nonintrusive optical visualization of surface nanobubbles," Physical Review Letters, vol. 109, 2012.
[35] C. U. Chan and C. D. Ohl, "Total-internal-reflection-fluorescence microscopy for the study of nanobubble dynamics," Physical Review Letters, vol. 109, 2012.
[36] J. Fritzsche and U. A. Peuker, "Wetting and Adhesive Forces on Rough Surfaces – An Experimental and Theoretical Study," Procedia Engineering, vol. 102, pp. 45-53, 2015.
[37] F. Heuzeroth, J. Fritzsche, and U. A. Peuker, "Wetting and its influence on the filtration ability of ceramic foam filters," Particuology, vol. 18, pp. 50-57, 2015.
[38] L. Ditscherlein, A. Schmidt, E. Storti, C. G. Aneziris, and U. A. Peuker, "Impact of the Roughness of Alumina and Al2O3-C Substrates on the Adhesion Mechanisms in a Model System," Advanced Engineering Materials, 2017.
[39] K. W. Stöckelhuber, "Stability and rupture of aqueous wetting films," European Physical Journal E, vol. 12, pp. 431-435, 2003.
[40] S. Calgaroto, K. Q. Wilberg, and J. Rubio, "On the nanobubbles interfacial properties and future applications in flotation," Minerals Engineering, vol. 60, pp. 33-40, 2014.
[41] A. Sobhy and D. Tao, "Nanobubble column flotation of fine coal particles and associated fundamentals," International Journal of Mineral Processing, vol. 124, pp. 109-116, 2013.
[42] R. Etchepare, H. Oliveira, M. Nicknig, A. Azevedo, and J. Rubio, "Nanobubbles: Generation using a multiphase pump, properties and features in flotation," Minerals Engineering, vol. 112, pp. 19-26, 2017.
[43] M. Zhang and J. R. T. Seddon, "Nanobubble–Nanoparticle Interactions in Bulk Solutions," Langmuir, vol. 32, pp. 11280-11286, 2016/11/01 2016.
[44] M. Cournil, F. Gruy, P. Gardin, and H. Saint-Raymond, "Modelling of solid particle aggregation dynamics in non-wetting liquid medium," Chemical Engineering and Processing: Process Intensification, vol. 45, pp. 586-597, 2006.
[45] P. Knüpfer, L. Ditscherlein, and U. A. Peuker, "Nanobubble enhanced agglomeration of hydrophobic powders," Colloids and Surfaces A: Physicochemical and Engineering Aspects, vol. 530, pp. 117-123, 10/5/ 2017.
[46] F. Gruy, M. Cournil, and P. Cugniet, "Influence of nonwetting on the aggregation dynamics of micronic solid particles in a turbulent medium," Journal of Colloid and Interface Science, vol. 284, pp. 548-559, 2005.
[47] C. Voigt, L. Ditscherlein, E. Werzner, T. Zienert, R. Nowak, U. Peuker, et al., "Wettability of AlSi7Mg alloy on alumina, spinel, mullite and rutile and its influence on the aluminum melt filtration efficiency," Materials and Design, vol. 150, pp. 75-85, 2018.
[48] M. Cournil, F. Gruy, P. Gardin, and H. Saint-Raymond, "Experimental Study and Modeling of Inclusion Aggregation in Turbulent Flows to Improve Steel Cleanliness," physica status solidi (a), vol. 189, pp. 159-168, 2002/01/01 2002.
[49] A. Agarwal, W. J. Ng, and Y. Liu, "Principle and applications of microbubble and nanobubble technology for water treatment," Chemosphere, vol. 84, pp. 1175-1180, 2011.
[50] Y. Wang and B. Bhushan, "Boundary slip and nanobubble study in micro/nanofluidics using atomic force microscopy," Soft Matter, vol. 6, pp. 29-66, 2009.
[51] L. Zhang, Y. Zhang, X. Zhang, Z. Li, G. Shen, M. Ye, et al., "Electrochemically controlled formation and growth of hydrogen

DIFFERENTIATING MATERIAL COMPOSITIONS USING LATERAL FORCE MICROSCOPY

WENQING SHI, JOHN PAUL PINEDA, BYONG KIM, AND KEIBOCK LEE
PARK SYSTEMS INC., SANTA CLARA, CA USA

Abstract

Nanoscale frictional measurement, or nanotribology, is an effective approach to identify surface compositional differences for a wide variety of materials, including polymer blends, thin films and semiconductors. Lateral Force Microscopy (LFM), a derivative mode in Atomic Force Microscopy (AFM), is particularly powerful in identification and mapping of the relative difference in frictional characteristics with superior spatial resolution. In this study, two samples with heterogeneous surface compositions, i.e., Sample 1 that consisted of polymer on glass and Sample 2 which contained graphene on Si, were analyzed with LFM, a mode that comes standard in all AFM systems from Park Systems. In Sample 1, homogeneously distributed circular features within the sample were seen from the topography, and the two materials, i.e., polymer and glass, were not easily distinguishable. However, two components with dramatically different frictional properties were clearly observed from the LFM images, which is indispensable to discriminate the two materials. In Sample 2, graphene and Si were differentiated unambiguously from the LFM signal, whereas the difference between the two materials from the topography result is relatively weak. Our results in this report showcased that LFM is ideal to analyze samples which consist of heterogeneous compositions with different frictional coefficients, while the topography is relatively flat.

Introduction

In past decades, nanoscale frictional force measurements have attracted great attention due to the needs for high resolution mechanical characterization of many newly-developed materials. Lateral force microscopy (LFM), [1] which is particularly useful for identifying and mapping heterogeneities in surface frictional characteristics, has found a steadily increasing number of applications, such as identification of different components within polymer blends and composites, mechanical testing of micro- and nanoelectrochemical systems (MEMS/NEMS) and delineation of surface coverages of deposited materials on thin films. [2-7]

Herein, we demonstrate the utility of LFM with Park atomic force microscopy (AFM) to identify surface compositional differences of two samples. First, as a proof-of-concept experiment, a sample that contained a polymer deposited onto a glass substrate was imaged with LFM. A clear difference in frictional characteristics was seen from the LFM measurements, albeit the two different frictional domains seen in the LFM images were obscured in the sole topography image. Next, graphene grown on Si was examined with LFM and scanning thermal microscopy (SThM) to examine both the frictional as well as the thermal properties of the sample. Interested readers can refer to Park AFM webpage on SThM for more detailed information regarding SThM mode. From the results, we observed clear difference in frictional and thermal behaviors between graphene and Si, which is far less pronounced in the topography image.

Experimental
Principle of LFM

The mechanism of LFM is very similar to that of Contact Mode. In Contact Mode, the deflection of the cantilever in the vertical direction is measured and utilized to generate surface topography. However in LFM, the deflection of the cantilever in the horizontal direction is measured instead. The lateral deflection of the cantilever occurs as a result of the force encountered by the cantilever as it moves horizontally across the sample surface. Factors that determine the magnitude of this deflection include: the frictional coefficient, the topography of the sample surface, the direction of the cantilever movement, and the cantilever's lateral spring constant.

In the operation of LFM, the cantilever movement in both the vertical direction and the horizontal direction is tracked via a position sensitive photo detector (PSPD) that consists of four domains (a quad-cell), shown in Figure 1. To obtain the surface topographical information, a "bi-cell" signal that is related to the difference between the upper cells (A+C) and the lower cells (B+D) measured from the quadrant detector is used (Equation 1), frequently referred to as an "A-B" signal.

Topographic information = (A+C) - (B+D) (Equation 1)

On the other hand, to get the surface frictional characteristics, the LFM signal is obtained from the difference between the right cells (A+B) and the left cells (C+D) (Equation 2).

Frictional information = (A+B) - (C+D) (Equation 2)

To provide a more direct illustration of how LFM works, the schematic illustration of cantilever deflection while the cantilever is scanning over a surface with different
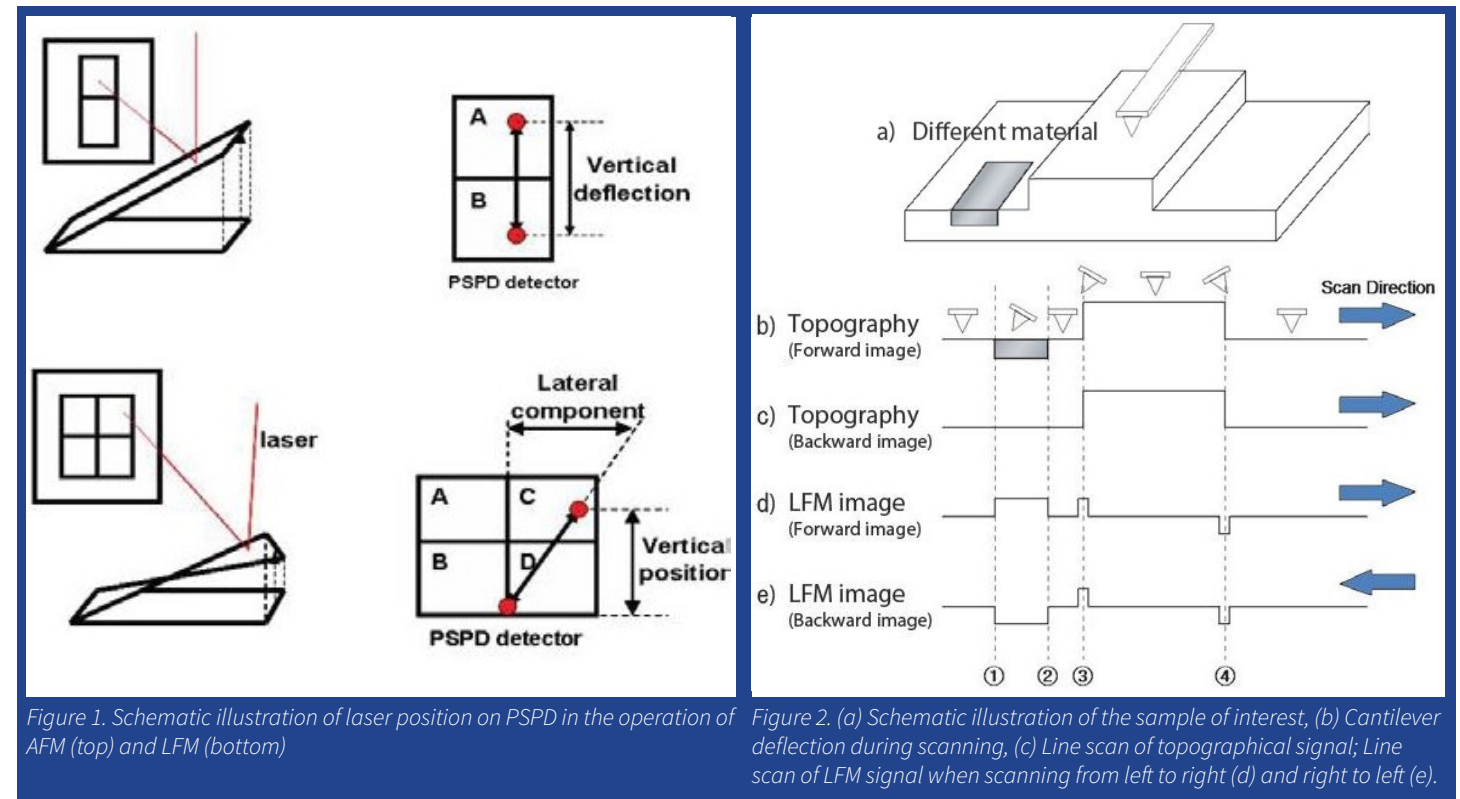

Figure 1. Schematic illustration of laser position on PSPD in the operation of AFM (top) and LFM (bottom)

Figure 2. (a) Schematic illustration of the sample of interest, (b) Cantilever deflection during scanning, (c) Line scan of topographical signal; Line scan of LFM signal when scanning from left to right (d) and right to left (e).

frictional domains is depicted in Figure 2. The surface structure used herein contains a raised step in the center and smooth areas on either side, with a region of higher frictional coefficient located at the flat part on the left (Figure 2a). The deflection of the cantilever as it traverses over the surface and encounters topographical features as well as heterogeneous frictional domains is shown in Figure 2b. A representative line profile of AFM topographical signal can be found in Figure 2c. Although the topographical information is the same between point 1 and point 2, a clear difference can be seen from the LFM signal (Figure 2d and 2e). The cantilever will tilt to the right as it scans from left to right over this region due to an increase in relative friction, which leads to an increase in the LFM signal. Whereas the cantilever will tilt to the left when the scan direction is reversed, and a decrease in LFM signal will be observed. The power of LFM lies in its ability to identify different components within a sample based on frictional characteristics while the surface is relatively flat, which allows the user to gain additional information about the sample.

Procedure of AFM Imaging

Two samples were selected and imaged with a Park NX10 AFM at ambient conditions. The first sample consists of a polymer deposited on a glass substrate; hereafter refer to as Sample 1. The second sample contains graphene grown on Si; hereafter refer to as Sample 2. Images for Sample 1 were acquired in LFM Mode using a scan rate of 1.0 Hz. Images for Sample 2 were acquired in both LFM Mode and SThM Mode with a scan rate of 0.6 Hz. In LFM imaging, a NSC36-C cantilever (nominal spring constant k = 1 N/m) was used. In SThM imaging, a NanoThermal-10 (nominal spring constant k = 0.25 N/m) was used.

Results or Discussion
Polymer on Glass

To demonstrate the performance of the LFM mode by Park AFM, we first imaged Sample 1 as a proof-of-principle experiment, with the topography image, LFM images and the representative line profiles shown in Figure 3. Images were acquired at a pixel size of 256 × 256 and a scan size of 20 μm × 20 μm. From the AFM topography image (Figure 3a), we observed circular features with diameters ranging from 1 to 2 μm and heights of 20 to 200 nm within the sample. In Figure 3a, red arrows labeled as 1, 2, and 3 were added to three representative circular features for better illustration. In terms of the feature dimension, diameters of 1.72 μm, 1.41 μm, and 1.33 μm were measured for features 1, 2, and 3. The heights of each of the three features were 50.1 nm, 158.2 nm, and 42.1 nm, respectively. The distribution of such features is relatively homogeneous throughout the sample. In addition to the appearance of the circular features, we also observed slight height variations within the area under investigation, i.e., ΔZ = 29.2 nm between the two triangular cursors as indicated in Figure 3a.

LFM forward (Figure 3b) and backward (Figure 3c) images were captured simultaneously along with the topography image, through which the frictional characteristic of the sample can be obtained. The LFM images clearly revealed the compositional heterogeneity within the sample, and two domains with distinct frictional coefficients were observed.

To provide a more direct comparison of the signal, line profiles along the solid lines drawn in the topography image (red line in Figure 3a), the LFM forward image (green line in Figure 3b), and the LFM backward image (blue line in Figure 3d) were generated with the XEI software and the three traces are displayed in Figure 3d. From the line profiles obtained from the LFM forward scan (green line in Figure 3d) and backward scan (blue line in Figure 3d), we can have a qualitative idea regarding the frictional characteristic of the sample. In brief, a downward shift in the LFM signal was observed during the forward scan (green line in Figure 3d), indicating that the movement of the cantilever was hindered by the underlying substrate due to frictional force. The cantilever was dragged by the surface and eventually a backward torsion occurred as it scanned from left to right, which was then observed as a negative shift in the lateral
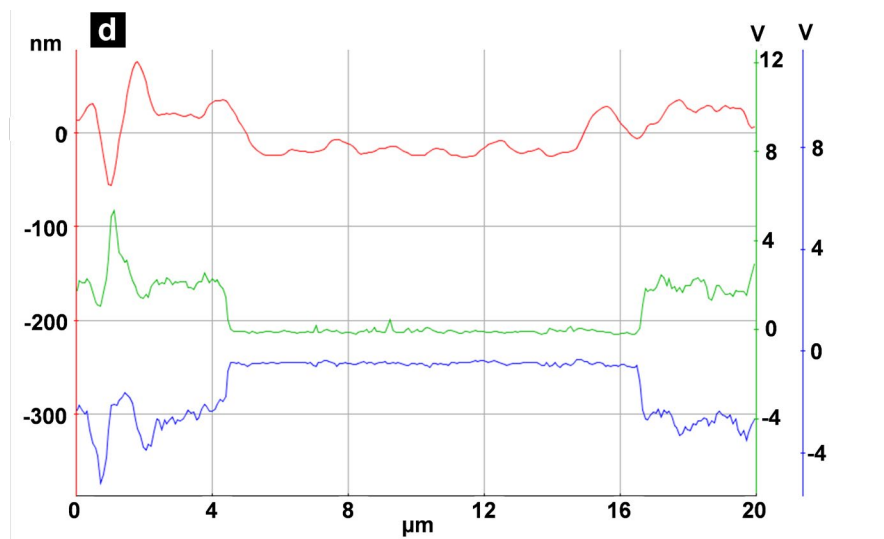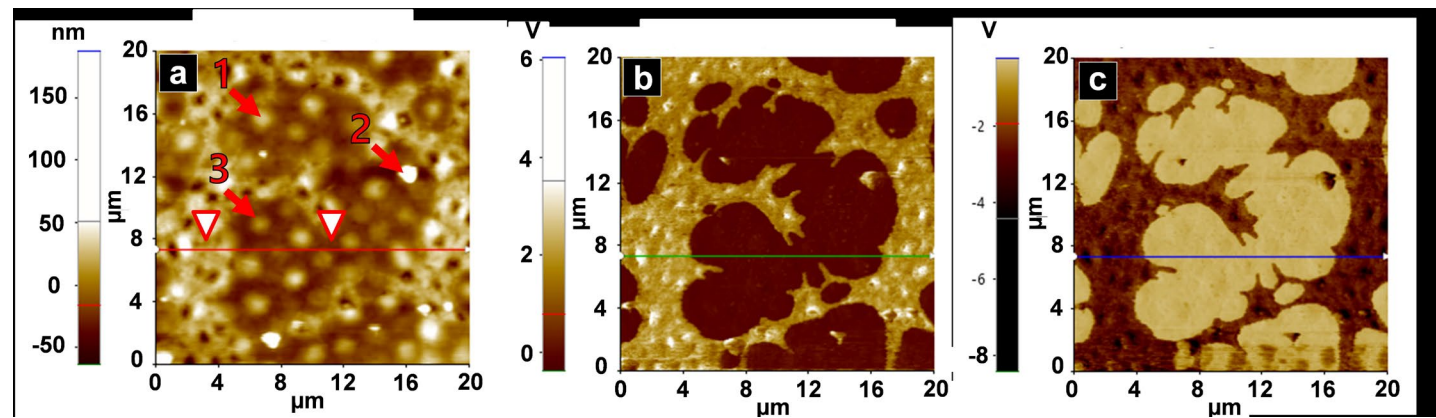
*Figure 3. (a) Topography image, red arrows were added to better illustrate representative circular features;
(b) LFM forward scan image;
(c) LFM backward scan image;
(d) line profiles plotted along the red line seen in 3a, green line seen in 3b and blue line seen in 3c, respectively.*
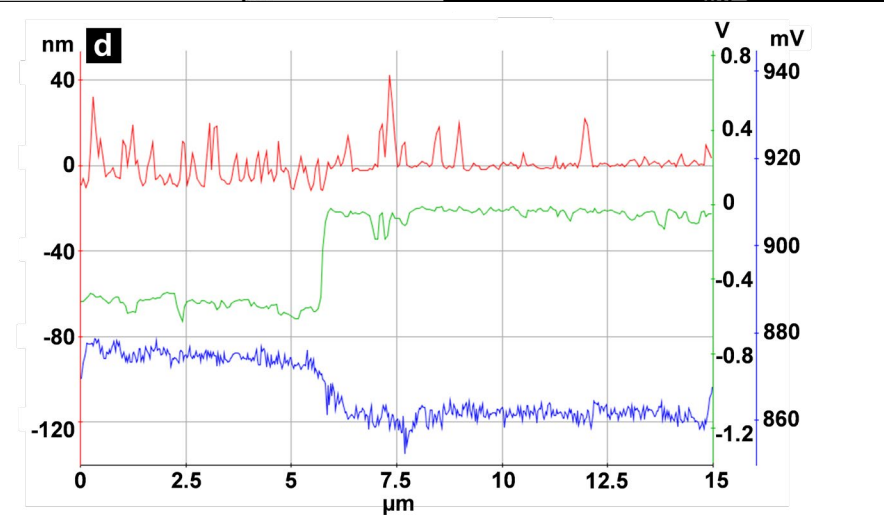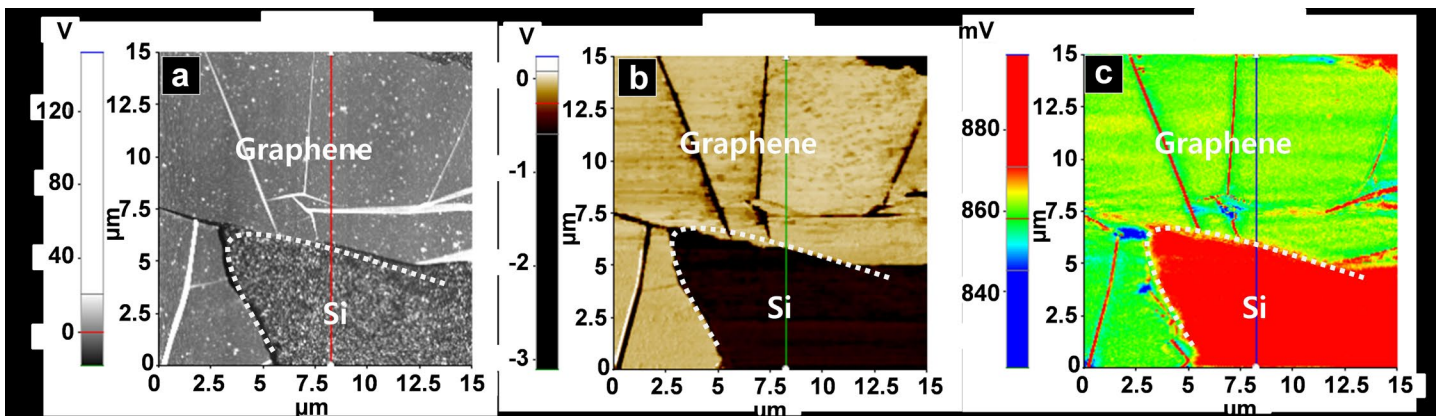

*Figure 4. (a) Topography image;
(b) LFM image and
(c) SThM image of Sample 2 (graphene on Si);
(d) Line profiles plotted along red line seen in 4a, green line seen in 4b, and blue line seen in 4c.*

deflection signal. Oppositely, the LFM signal shifted upwardly during the backward scan (blue line in Figure 3d), which, again, is a result of the cantilever being dragged by the surface because of the larger frictional interaction between the cantilever and the surface. As a result, we can conclude that the frictional coefficient for the central area is higher as compared to the surrounding areas.

Another interesting finding here is, although drastic changes were observed in both the green trace (LFM forward) and the blue trace (LFM backward), only minor height variations were seen in the red trace (topography). Results here showcased the strength of LFM to identify different components within a sample based on the frictional properties even when no significant difference can be seen from the topographical data.

Oppositely, the LFM signal shifted upwardly during the backward scan (blue line in Figure 3d), which, again, is a result of the cantilever being dragged by the surface because of the larger frictional interaction between the cantilever and the surface. As a result, we can conclude that the frictional coefficient for the central area is higher as compared to the surrounding areas.

Another interesting finding here is, although drastic changes were observed in both the green trace (LFM forward) and the blue trace (LFM backward), only minor height variations were seen in the red trace (topography). Results here showcased the strength of LFM to identify different components within a sample based on the frictional properties even when no significant difference can be seen from the topographical data.

Graphene on Si

Upon demonstration of the LFM operation with Sample 1, we then repeated the LFM measurements on Sample 2 to examine the difference in frictional characteristics between graphene and Si. In addition, we also conducted SThM imaging to study the thermal properties of

the two materials. Images were acquired with a pixel size of 256 × 256 and a scan size of 15 μm × 15 μm.

In Figure 4a, topography of Sample 2 is shown. The boundary between graphene and Si, as indicated by the white dashed line, is discernable. A representative line profile was plotted along the red line drawn in Figure 4a and is shown in Figure 4d (red trace), a ΔZ of ~5 nm was measured between graphene and Si. From the LFM image in Figure 4b, the two materials were clearly differentiated. From the line profile (green trace in Figure 4d) of the LFM signal, a larger frictional coefficient was observed for Si compared to that of graphene, as evident by the downward shift in the LFM signal over Si as compared to that over graphene. According to previous literature, the nominal friction coefficient for graphene is 0.03,[8] whereas the nominal friction coefficient for Si is 0.2.[9] Our LFM results are consistent with previous literature. Furthermore, to gain insights about the thermal properties of the two materials, SThM was performed, with the resultant SThM error image shown in Figure 4c and a representative line profile (blue trace) shown in Figure 4d. A higher SThM error was observed over Si than graphene, which indicates a higher thermal conductivity of graphene as compared to that of Si.

Conclusions

Here we demonstrate the use of LFM to differentiate surface compositional variations based on the relative differences in frictional properties. Implemented with Contact Mode AFM imaging, this technique enables nanoscale characterization of frictional domains within a sample. The strength of LFM is first demonstrated in Sample 1, where the two different materials (i.e., polymer and glass) within the sample were not easily distinguishable from the topography image. However, from the LFM images, the two domains were clearly separated by their difference in frictional coefficient. Next, we applied both LFM and SThM to examine the frictional as well as thermal properties of Sample 2, which is

graphene grown on Si. Qualitative results show that graphene has a lower frictional coefficient and a higher thermal conductivity as compared to that of Si. In conclusion, LFM has already found a wide range of applications in nanoscale frictional measurements and will continue to facilitate the development of many exciting technologies.

References

1. Mate, C. M., McClelland, G. M., Erlandsson, R., & Chiang, S., Atomic-scale friction of a tungsten tip on a graphite surface. Phys. Rev. Lett., 1987, 59, 1942.
2. Sheiko, S. S. Imaging of polymers using scanning force microscopy: from superstructures to individual molecules. New Developments in Polymer Analytics II. Springer Berlin Heidelberg, 2000. 61-174.
3. Perry, S. S. Scanning probe microscopy measurements of friction. MRS bulletin, 2004, 29, 478-483.
4. Perry, S. S., & Tysoe, W. T. Frontiers of fundamental tribological research. Tribology Letters, 2005, 19, 151-161.
5. Munz, M., Schulz, E., & Sturm, H., Use of scanning force microscopy studies with combined friction, stiffness and thermal diffusivity contrasts for microscopic characterization of automotive brake pads. Surface and interface analysis, 2002, 33, 100-107.
6. Raczkowska, J., Montenegro, R., Budkowski, A., Landfester, K., Bernasik, A., Rysz, J., & Czuba, P., Structure evolution in layers of polymer blend nanoparticles. Langmuir, 2007, 23, 7235-7240.
7. Sun, S., Chong, K. S., Leggett, G. J., Photopatterning of self-assembled monolayers at 244 nm and applications to the fabrication of functional microstructures and nanostructures. Nanotechnology, 2005, 16, 1798.
8. Shin, Y. J., Stromberg, R., Nay, R., Huang, H., Wee, A. T., Yang, H., & Bhatia, C. S., Frictional characteristics of exfoliated and epitaxial graphene. Carbon, 2011, 49, 4070-4073.
9. Deng, K., Ko, W. H., A study of static friction between silicon and silicon compounds. Journal of Micromechanics and Microengineering, 1992, 2, 14.

AN IN DEPTH LOOK AT IMPLANTABLE ORGANIC NANO ELECTRONICS

Dr. Tobias Cramer, Asst. Professor and Researcher at University of Bologna, Italy

BIOELECTRONIC INTERFACES OFFER MANY POTENTIAL MEDICAL BREAKTHROUGHS INCLUDING RESTORING HEARING, CREATING ARTIFICIAL RETINAS TO RESTORE EYESIGHT AND MANY OTHER NEURAL ADVANCES FOR LOST NERVE FUNCTIONS BY CREATING PARTICULAR DEVICES FOR SPECIALISED REGIONS OF THE NERVOUS SYSTEM, IN ORDER TO COMPENSATE FOR THE LOSS OF FUNCTION.
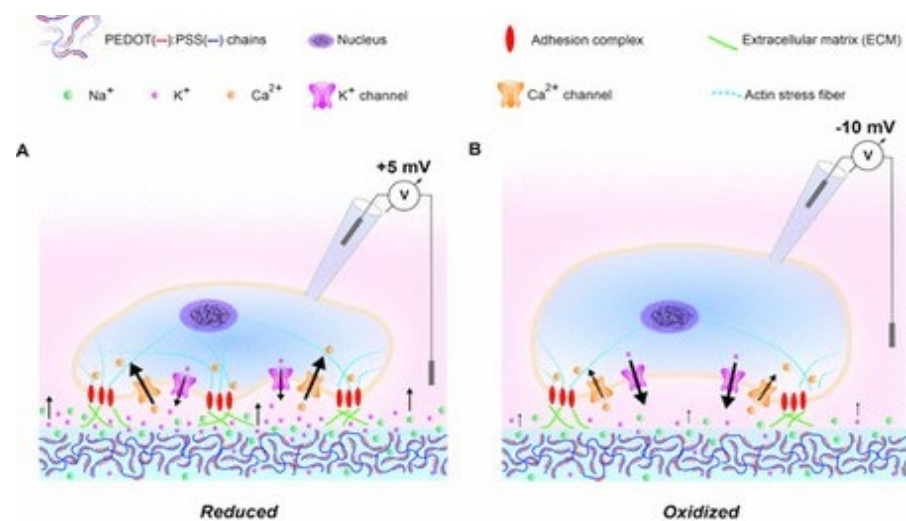
Dr. Tobias Cramer, Asst. Professor and Researcher at University of Bologna, Italy. Professor Cramer works in the semiconductor physics group at University of Bologna, Italy with a focus on flexible and stretchable semiconductors for bioelectronics and photonic applications. He teaches the course "Laboratory of Nanoscience and Technology" in the Master Degree "Materials Physics and Nanoscience (MANO)" He is responsible for the Atomic Force Microscopy lab and development of stretchable sensors for bioelectronics.

Tobias Cramer studied chemistry and physics at the University of Freiburg (D) and finished in 2006 with a Ph.D. degree. After a period of post-doctoral fellowships with stays in Germany (Institute for Advanced Studies, Freiburg), Italy (Faculty of Chemistry and Institute for the Study of Nanostructured Materials – ISMN-CNR, both Bologna) and United States (The Scripps Research Institute, San Diego). Since 2014, he has worked as a researcher in the Department of Physics and Astronomy at UNIBO, where he is a tenure track professor. In his research he investigates nano-scale charge transport phenomena in condensed matter by theoretical and experimental methods. He is the author of 45 scientific articles and book chapters.

Flexible, biocompatible electronic materials and semiconductors are wanted to create a novel generation of bioelectronic interfaces. Such interfaces will be at the heart of future medical devices that allow to record and stimulate in a low-invasive manner from the central and peripheral nervous system or to transduce directly biochemical signals. In their research they investigate in detail the material properties and the underlying physics of novel material candidates for bioelectronic interfaces. The experiments provide them the necessary knowledge to propose novel transducer concepts that could help to improve the interface between the worlds of biological cells and microelectronics.

IN OUR GROUP WE EMPLOY A PARK NX10 AFM EQUIPPED WITH DIFFERENT MODULES ALLOWING FOR MULTI-MODAL AFM TECHNIQUES.

Reduced   Oxidized

IMPLANTABLE ORGANIC NANOELECTRONICS

An Interview with Tobias Cramer, Asst. Professor, Department of Physics and Astronomy, University of Bologna, Italy

Professor Cramer works in the semiconductor physics group at University of Bologna, Italy with a focus on flexible and stretchable semiconductors for bioelectronics and photonic applications. He teaches the course "Laboratory of Nanoscience and Technology" in the Master Degree "Materials Physics and Nanoscience (MANO)" He is responsible for the Atomic Force Microscopy lab and development of stretchable sensors for bioelectronics.

Pictured (far right): Dr. Cramer with the Bologna Semiconductor Physics Group, physicists doing research on semiconducting materials at University of Bologna. See all their research at their new website: https://site.unibo.it/semiconductor-physics/en/research/organic-bioelectronics

Can you give a brief overview of Implantable Organic NanoElectronics (IONE) and describe the benefits?
In recent years materials based on organic small molecules or polymers have been developed that combine important properties of two rather different material classes: On the one hand they show semiconducting electronic properties equivalent to materials employed in modern information and communication technology. On the other hand they also have soft and biocompatible properties as well as stability in water, all typical for biomaterials. IONE employs such materials to develop novel microelectronic implants that interface to important processes in the body, relevant to diagnose or treat disease.

How are implantable organic nano electronics inspired by nature?
Information in the nervous system is processed as electronic excitations in nerve cells. The underlying microscopic mechanisms build on the cell's ability to control tiny ionic current fluxes. The immense relevance of ion transport processes in Nature stimulates the research done for IONE. Modern information and communication technology materials control electronic excitations and currents in a very precise way, but ionic mechanisms do not play any role. IONE is changing this paradigm and some novel organic materials show efficient ionic as well as electronic transport. This opens also new opportunities to build improved bioelectronic interfaces.

How are IONE different from bioelectronics?
IONE is developing new means to perform bioelectronic research or to interface to bioelectronic systems. With the help of organic nanomaterials less invasive interfaces are developed that permit a two-directional communication with the neuronal system. Recording with such interfaces will allow us to intercept the body's communication channels. Stimulation instead allows us to impact on them.

Can you explain how they can be used in Human Technology interfaces and give some examples?
The materials that we are investigating are designed to build less invasive interfaces with the nervous system that could operate in chronic conditions. That means during normal activity the IONE microdevices are able to record signals from the body and analyse them continuously without interference or impact on the body's own processes. Such a recording technology will help to increase our knowledge about the bioelectronic signaling processes in the human body in a much more precise way. For example, there is currently only a rough understanding that the peripheral nervous system is also responsible for immune response and inflammation. A precise understanding and then the possibility to impact on the related signals by stimulation could provide new means to treat disease states locally and without pharmaceuticals.

Can you describe the latest discovery of Direct electrical neurostimulation with organic pigment photocapacitors and why this is important research?
This research regards an organic nanomaterial that has been invented by Eric Daniel Glowacki at Linköping University. As Physicists we investigate in detail the microscopic mechanism that occurs when such materials are illuminated by a strong red light source. And it is remarkable. Although it consists of a layer of only a few tens of nanometers, it leads to the efficient generation of a charged bilayer. The resulting transient ionic current pulse is sufficiently strong to excite neuronal cells. So this material is becoming a very hot candidate for artificial retina implants. With this device no battery support or wiring with cables will be necessary. The light pulse will provide
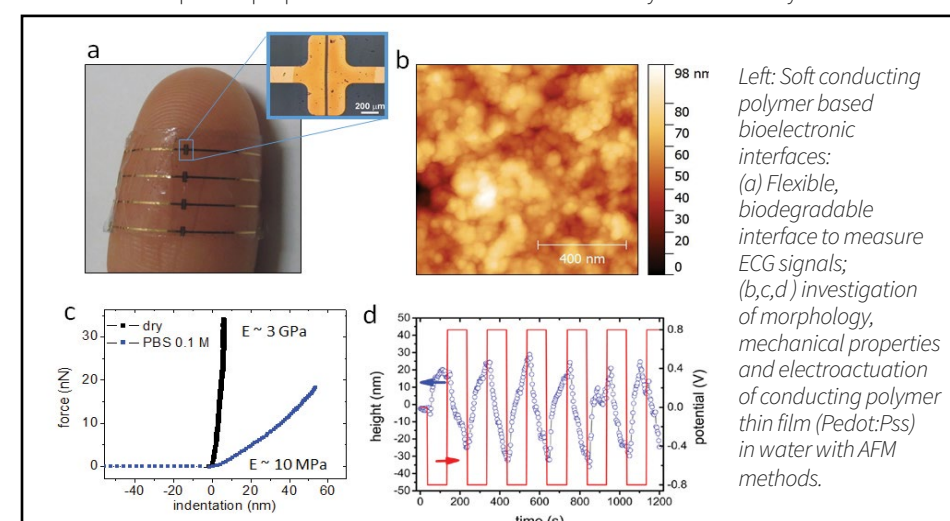
Left: Soft conducting polymer based bioelectronic interfaces: (a) Flexible, biodegradable interface to measure ECG signals; (b,c,d) investigation of morphology, mechanical properties and electroactuation of conducting polymer thin film (Pedot:Pss) in water with AFM methods.

enough energy to excite the visual nerve locally, potentially making such implants much more simple and less invasive.

Can you describe the potential for use in space environments to reduce damage from ionizing radiation?

This relates to a different class of semiconducting materials that we are investigating in our lab. For the space environment we need semiconductors that show an enormous chemical and structural stability. The problem is that in space, everything is subjected to large amounts of ionizing radiation. Organic electronics for example seems to degrade earlier under such conditions. So for that purpose we investigated amorphous oxide based semiconductors. Similar to organic materials amorphous oxides can be patterned on large areas and on flexible substrates leading to bendable, large area electronic devices. Now for the space environment, oxide electronics have the big advantage that they are highly resistant to ionizing radiation as we demonstrated with our research work.

How is AFM used in your research?

We have many different applications for AFM. In fabrication work we use it a lot in routine investigations of surface morphology and layer thickness. But what I like about AFM is its versatility. Multimodal techniques provide much more information than just morphology. For the research of novel electronic materials this is fundamental. For example with KPFM we can measure now in detail how the electronic transport properties of our semiconductors layers vary while we start to apply tensile strain to the material and stretch it.

What other advances do you see in the field of IONE? Give some future predictions.

First of all, we still have to focus our efforts to bring organic nanomaterials to real clinical applications. Currently we have demonstrated impressing proof of principles, but to push these concepts forward into real improvements for patients will take more energy. Then of course also for the future I can imagine some promising developments for organic nanoelectronics. Of course our dream is to extent technological information processing into 3D by using our novel materials, but that is another story …

You are teaching a course called, "LABORATORY OF NANOSCIENCE AND NANOTECHNOLOGY". Do you think students today view science drastically differently, compared to students who studied science before the Nanotechnology boom in the 1980s?

Yes of course it is different and that is the reason why we recently introduced the new master course "Materials Physics and Nanoscience" at our University in Bologna.

At first sight one would think that students just have to learn more and more, but I think this is not the case. Focus has to be set on important concepts and one also has to take experimental skills seriously. Regarding the recent developments in equipment it has also become easier to teach nanoscience. For example nowadays it is no problem that students perform their own AFM experiments independently in the laboratory course.

What Students Say about the course:

"I didn't expect to work on my own with an AFM in a laboratory course. It helped me a lot to figure out how AFM works in practice and it was very motivating." Matteo Verdi, MANO student, University of Bologna 2018

"The laboratory of nanoscience and technology course was fantastic: it provided us with the basic knowledge about nanoscience. We also had a lot of opportunities to get into contact with real research problems." Giovanni Armaroli, MANO student, University of Bologna 2018

"THE AFM IS A CRUCIAL INSTRUMENT FOR THE BASIC QUALITY ASSURANCE ON OUR SAMPLES TO GET ACCURATE MEASUREMENTS ON MORPHOLOGY, THICKNESS, ETC." EXPLAINS DR. CRAMER, SEATED IN FROM ON OF THE PARK NX 10 AFM. "WE ALSO DO EXPERIMENTS THAT YOU CANNOT DO WITH OTHER EQUIPMENT USING AFM SUCH AS MEASURING IMPORTANT MECHANICAL AND ELECTRICAL INTERACTIONS AT THE NANOSCALE."

In our group we employ a Park NX10 AFM equipped with different modules allowing for multimodal AFM techniques.
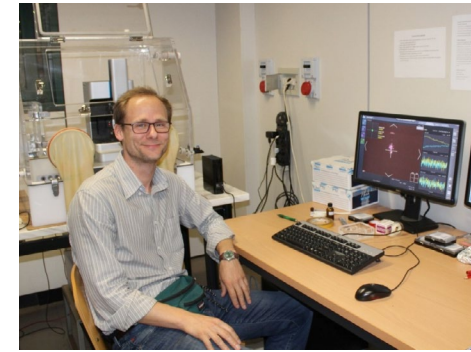
Soft bioelectronic devices that interface non-invasively neuronal tissue are expected to open an enormous potential for novel medical therapies.
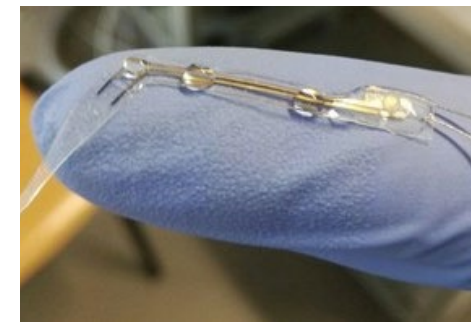
This technology encounters a fundamental limit as a compromise between mechanical stability and the medical invasiveness has to be found: Bioelectronics interfaces should match the soft elastic properties of the tissue where they are embedded (E < 1 MPa). Missing compliance with the low elastic modulus of tissue leads on the long-term to inflammation, scar formation and passivation. However, bio-electronic implants rely on patterned microelectronic structures made of more rigid electronic materials for signal recording and stimulation. The resulting mismatch in mechanical properties imposed by the requirement of a soft substrate combined with electrical functional rigid elements makes bio-electronic microelectrodes prone to stress induced mechanical failure and does not allow any further miniaturization and reduction in invasiveness.

To overcome the fundamental limitations in the engineering of soft, multi-component microelectronic devices, Dr. Cramer's group investigates novel materials and device architectures that combine soft mechanical behaviour with stable electronic performance. They employ a wide range of macroscopic and microscopic techniques to decipher the combined electromechanical effects relevant for bioelectronic interfaces.
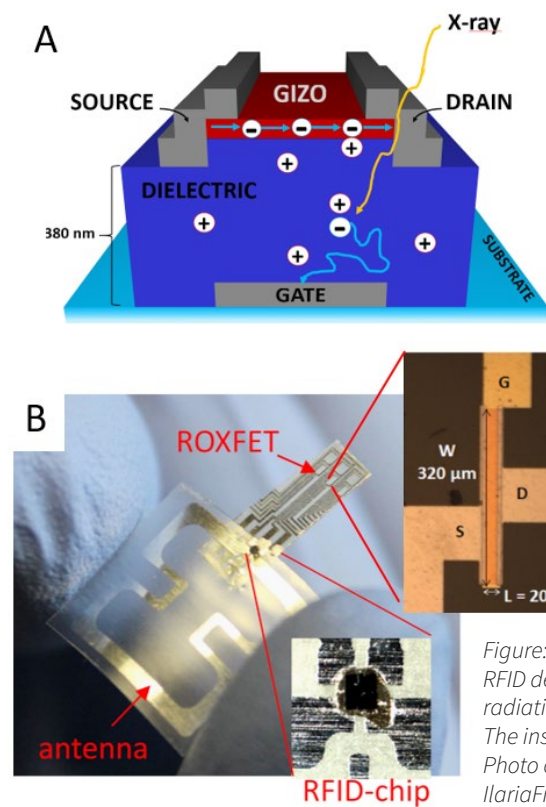

Figure: Novel microelectronic X-ray dosimeter compatible with flexible plastic substrates and passive RFID detection A) Scheme showing the operation mechanism of the dosimeter that employs a radiation sensitive oxide field effect transistors (ROXFET) B) Photo showing the wireless RFID sensor. The insets show micrographs of the RFID chip and of the ROXFET microelectronic dosimeter. C) Photo of the UNIBO team working on the project (from left to right: Tobias Cramer, Beatrice Fraboni, IlariaFratelli).

Wireless, flexible, low-power and real-time microelectronic X-ray dosimeters

Authors and affiliations: Tobias Cramer[1]*, Ilaria Fratelli[1], Pedro Barquinha[2], Ana Santa[2], Cristina Fernandes[2], Franck D'Annunzio[3], Christophe Loussert[3], Rodrigo Martins [2], Elvira Fortunato[2], Beatrice Fraboni[1]

1. Department of Physics and Astronomy, University of Bologna, VialeBertiPichat 6/2, 40129 Bologna, Italy.
2. CENIMAT/I3N and CEMOP-UNINOVA, Departamento de Ciência dos Materiais, Faculdade de Ciências e Tecnologia, Universidade NOVA de Lisboa, Campus de Caparica, 2829-516 Caparica, Portugal.
3. Tagsys Rfid, 785 Voie Antiope, 13600 La Ciotat, France.

Introduction:

Exposure to ionizing radiation such as x-rays or γ-rays may alter the atomic and molecular structure of materials and biological compounds representing a threat to human health as well as to electronic devices, as the modifications induces by irradiation can cause cancer in humans or failure in devices. To avoid health or technical safety risks the exposure to ionizing radiation has to be tightly controlled in a wide range of applications that span from medical radiotherapy and nuclear waste management to high energy physics experiments and space missions. .Currently available radiation dosimeters that provide information in real-time are designed as high precision devices, but are often expensive and with rather large and bulky shapes. In order to continuously monitor radiation exposure, low-cost and non-invasive microelectronic dosimeters are highly wanted.

Traditional microelectronic materials such as crystalline silicon cannot easily meet the application requirements of microelectronic dosimeters for two reasons: First, they do not absorb sufficient amounts of high energy radiation to be sensitive as they contain mostly elements with a rather low or medium atomic number Z. Second, as crystalline materials, they are fabricated on rigid wavers and cannot be patterned onto flexible plastic foils.

Results:

In order to overcome these limitations our research team has been investigating amorphous oxide semiconductors as novel materials for microelectronic dosimeters. Oxide semiconductors based on Indium Gallium Zink Oxide (IGZO) have the right structural and electronic properties to achieve fast transport of electrons as a n-type semiconductor even in the case of an amorphous, that is disordered, microstructure. This opens the way to deposit the IGZO semiconductor by physical methods on large flexible substrates instead of relying on crystalline growth. For our research on microelectronic dosimeters, we combined the IGZO transistors with a high-Z oxide dielectric that absorbs the ionizing radiation and builds up a space charge layer. The combined device structure, that we call radiation sensitive oxide field effect transistor (ROXFET), is shown in Figure 1. By introducing the amorphous oxide based semiconductor, we achieve a microelectronic dosimeter that outperforms similar silicon based devices by an order of magnitude in sensitivity achieving the detection of radiation doses down to the 100 μGy range. In addition, we demonstrate that the dosimeter can be patterned in arrays on flexible plastic foil. The fast electronic transport properties of IGZO make it also possible to integrate the ROXFET in a passive RFID circuit. With support from the French company Tagsys-RFID we created the first wireless radiation sensor that operated without a battery. Its detection mechanism is so energy efficient, that a radio frequency signal as generated by an RFID reader provides enough energy to operate the sensor and to send back to the reader the information on the sensor irradiation status.

The research has been carried out in collaboration with the group of Prof. Rodrigo Martins of the Universidade Nova di Lisbon (PT) and the results have been recently patented and published in Science Advances.Our results pave the way towards a new generation of flexible, real-time and low-power microelectronic dosimeters able to provide continuous, non-invasive and fully passive monitoring of ionizing irradiation exposure, e.g. during medical radiotherapy or during space mission to monitor exposure during radiotherapy or radiation damage in electronics. To find full article go to: http://advances.sciencemag.org/content/4/6/eaat1825

SIMULTANEOUS TOPOGRAPHICAL AND ELECTROCHEMICAL MAPPING USING SCANNING ION CONDUCTANCE MICROSCOPY
– Scanning Electrochemical Microscopy (SICM-SECM)

WENQING SHI, CATHY LEE, GERALD PASCUAL, JOHN PAUL PINEDA, BYONG KIM, KEIBOCK LEE, PARK SYSTEMS INC., SANTA CLARA, CA USA

Introduction

Since the inception of scanning tunneling microscopy (STM) [1], electrochemists have sought to take advantage of scanned probe microscopy (SPM) techniques to manipulate the spatial position of a probe with high resolution to facilitate simultaneous high resolution topographical, conductometric, and amperometric/voltammetric imaging of surface and interfaces [2]. Lately, scanning ion conductance microscopy (SICM) [3], has emerged as a versatile non-contact imaging tool and been employed for a variety of applications. SICM has been used to investigate the surface topography of both synthetic and biological membranes [4, 5], ion transport through porous materials, dynamic properties of living cells [6, 7, 8], and suspended artificial black lipid membranes [9]. In addition, integration of complementary techniques with SICM has led to many exciting new applications, including scanning near-field optical microscopy (SNOM) [10] and patch-clamping [11, 12]. Powerful as it is, SICM remains insensitive to electrochemical properties, or, in other words, SICM is inherently chemically-blind and has no chemical specificity.

To obtain spatially-resolved electrochemical information, scanning electrochemical microscopy (SECM), also known as the chemical microscope, has been developed. SECM has been widely employed to examine localized electrochemical properties and reactivity of various materials/interfaces, such as electrode surfaces and interfaces [13, 14, 15], membranes [16, 17, 18], and biological systems [19, 20, 21, 22, 23]. Despite its many applications, SECM, however, lacks reliable probe-sample distance control, and the probe is usually kept at a constant height during conventional SECM scanning. As a result, any variation in surface topography will result in changes in

probe-sample distance, and thus leading to convolution to the measured faradaic current, which will complicate the subsequent data interpretation [18].

To address the above-mentioned issues for SICM and SECM, hybrid SICM-SECM techniques have been developed, in which the SICM compartment provides the accurate probe-sample distance control, while the SECM compartment measures the faradaic current for electrochemical information collection. Here in this application note, first, the principle of operation for SICM, SECM and SICM-SECM will be briefly discussed. Next, the probe as well as the sample that are used for SICM-SECM imaging experiments are described. Finally, simultaneous SICM-SECM topography imaging and electrochemical mapping with SmartScan RTM10e using a Park NX12 AFM system is demonstrated.

Principle of Operation

Scanning Ion Conductance Microscopy (SICM)

In SICM operation, an electrolyte-filled nanopipette is used as the probe to raster scan an underlying substrate immersed in bath electrolyte (i.e., PBS buffer). A Ag/AgCl electrode is back-inserted in the pipette to serve as the working electrode, while another Ag/AgCl electrode is placed in the bath solution and used as the reference electrode. As a potential is applied between the two electrodes, an ion current is generated. The amplitude of the ion current is probe-substrate distance (Dp-s) dependent. The ion current decreases as the probe approaches the sample surface. This is a result of the ion flow being hindered between the probe tip and the underlying surface. This current-distance relationship can be obtained experimentally with an approach curve, where the ion current is plotted as a function of Dp-s.

At every recorded Dp-s, a specific ion current is measured. This distance-dependent ion current is then used as a feedback to control probe position during scanning. As a result, the topographical map of the substrate under study is generated. However, the major cavity in the capability of SICM is its lack of chemical specificity.
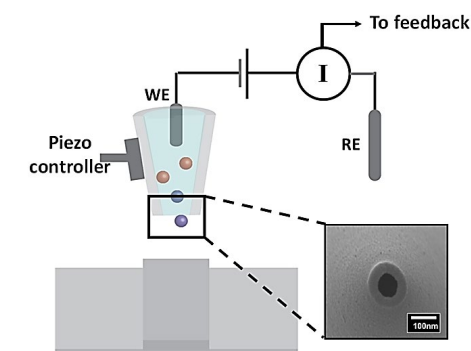
Fig. 1 SICM schematic illustration. The scanning probe consisted of a working electrode (WE, Ag/AgCl) back-inserted into a nanopipette. The reference electrode (RE) is placed in the bath solution (i.e., PBS buffer). The nanopipette opening is shown in the zoomed-in scanning electron micrograph. As a potential is applied between the WE and RE, a distance-dependent ion current is generated, based on which a piezoelectric positioner is used to maintain a constant probe-substrate distance during scanning. As a result, topographical information of the sample under study can be obtained.

### Scanning Electrochemical Microscopy (SECM)

Scanning electrochemical microscopy employs a micro- or nanoelectrode, termed as the tip, to scan in the vicinity of a substrate. The bath solution consists of supporting electrolytes and an electrochemically active species. During a SECM experiment, the tip is biased at a sufficient potential such that the electrochemical active

species. During a SECM experiment, the tip is biased at a sufficient potential such that the electrochemical active species will either be oxidized or reduced at the tip. By measuring the faradaic current, quantitative electrochemical information of the interfacial region will be obtained. Several imaging schemes have been developed for SECM operation, including negative feedback mode, positive feedback mode, and substrate generation/tip collection (SG/TC) mode. Feedback mode exploits the variation in the faradaic current as the tip approaches the substrate, with the sign (i.e., +/-) of the variation depending upon the conductivity of the surface. When the probe approaches a conductive surface, redox cycling will lead to an increase in the measured faradaic current, this is known as the positive feedback. Whereas if the probe moves close to an insulative surface, the diffusion of the redox molecules to the electrode surface will be hindered, and, thus, a decrease in faradaic current will be detected, also known as the negative feedback. In SG/TC mode, the sample and the tip are biased at different potentials, where the sample is biased to generate (oxidize or reduce) redox species in solution and the tip is biased to collect (reduce or oxidize) the species generated at the substrate.

Taken in total, the drawback in SECM lies in the fact that feedback-controlled probe positioning is complicated by the different faradaic current behavior over conductive and insulative substrates. In conventional SECM measurements, constant-height imaging is used, in which the tip is maintained at a constant height from the surface and the faradaic current is recorded. In constant-height SECM imaging, when variations in surface topography and reactivity occurs concurrently, the data interpretation becomes problematic.

Hybrid SICM-SECM

To overcome the limitations in constant-height SECM imaging, an alternative approach, SICM-SECM, has been developed. A number of pipette-based probes have been designed for SICM-SECM imaging. Bard and his colleagues have developed a gold-coated micropipette insulated with electrophoretic paint. [24] A similar approach has been reported by Hersam and his colleagues, in which the Au-coated pipette was first completely insulated with atomic layer deposition of Al2O3, followed by focus ion beam (FIB) milling to expose both the nanopore and gold electrode. [25] In an alternative approach, a theta pipette is used, with one barrel filled with electrolyte for SICM and the other barrel filled with pyrolyzed carbon for SECM. [26] In SICM-SECM operation, the probe-sample distance can be controlled via the SICM compartment and the electrochemical activity can be measured via the SECM compartment, enabling truly independent concurrent topographical and electrochemical imaging.
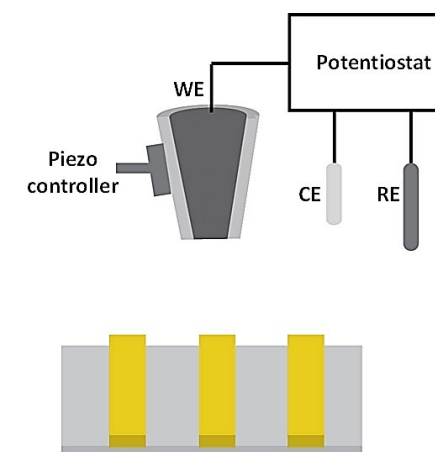

Experimental

Fig. 2 SECM schematic illustration. The electrochemical cell consisted of a working electrode (WE), a counter electrode (CE) and a reference electrode (RE). The bath solution contains supporting electrolyte and an electrochemically active species. During SECM operation, the WE is biased at a sufficient potential at which the redox reaction of the electrochemically active species occurs. By scanning the probe at a constant-height away from the underlying substrate while recording the faradaic current response, the electrochemical activity of the surface can be obtained.

Sample

As shown in Figure 3, the standard sample used for SICM-SECM experiment described herein consists of Au bars that are 10 μm in width and 300 nm in height on Pyrex substrate. The pitch width is 20 μm.
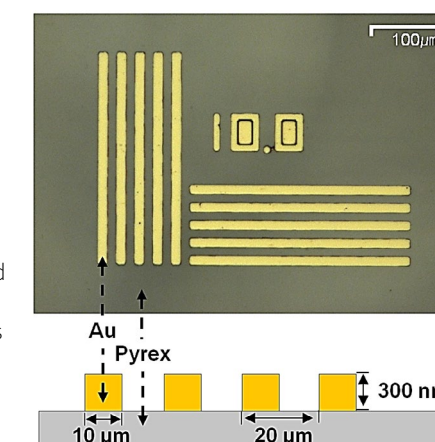
Fig. 3 SICM-SECM standard sample. The sample consisted of Au bars with a width of 10 μm and a height of 300 nm on Pyrex substrate. The pitch width is 20 μm.

Probe

The probe used herein is adopted from a method described in Shi et al. [18]. In brief, nanopipettes obtained via laser pulling were first coated with 10 nm Cr adhesion layer, followed

by 200 nm Au layer by thermal evaporation. Next, chemical vapor deposition of parylene C was performed such that the Au-coated nanopipettes were completely covered by parylene C. Finally, a focused ion beam (FIB) technique was used to expose the nanopore and the Au crescent. A representative scanning electron micrograph of the SICM-SECM probe is shown in Figure 4. The diameter of the central pore ranges from 200 – 250 nm. The Au crescent thickness is ~200 nm.
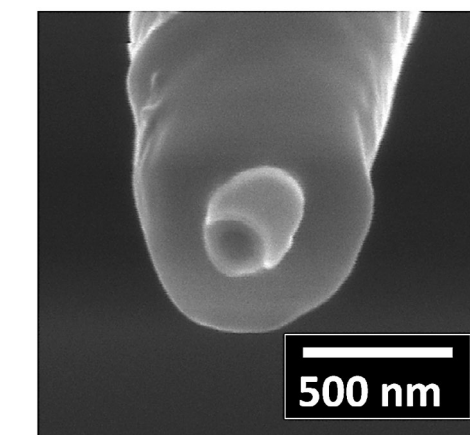

Cyclic Voltammetry

Fig. 4 Representative scanning electron micrograph of the SICM-SECM probe. Pore opening ~250 nm. Au crescent coating ~200 nm.

Prior to SICM-SECM imaging, cyclic voltammetry (CV) in a bulk solution consisted of 100 mM KCl and 10 mM Ru(NH3)63+ was performed. The purpose of the CV measurement is to 1) characterize the Au crescent electrode performance and 2) to choose the potential at which the Au crescent electrode will be biased at during SICM-SECM imaging experiments. To carry out the CV measurement, a potentiostat (Model 760E, CH instrument, Austin, TX) with a three-electrode electrochemical cell is used. The Au crescent electrode served as the working electrode (WE) with respect to a Ag/AgCl reference electrode (RE) and a Pt counter electrode (CE) in the bulk solution, as indicated in the cartoon illustration seen in Figure 5a.
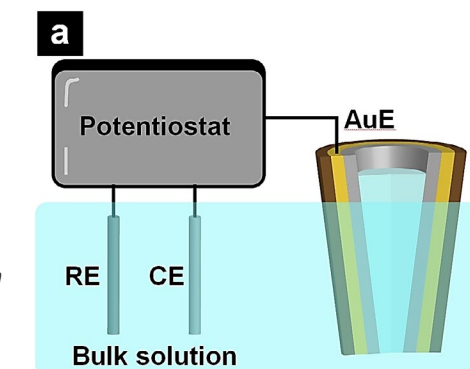
Fig. 5 a) Cartoon illustration of CV measurement; b) Setup of the CV measurement performed with the probe mounted on the SICM head of a Park NX12 AFM system.
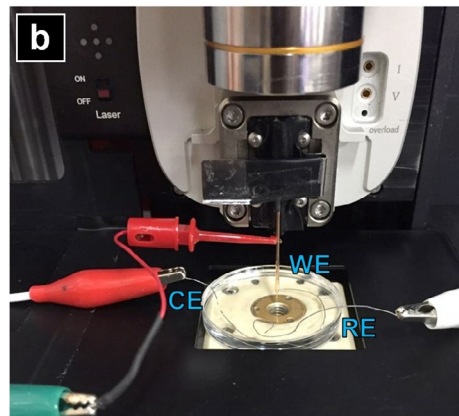
In Figure 5b, setup of the CV measurement performed with the probe mounted on the SICM head of a Park NX12 AFM system is shown. The potential window used here is from 0 to -0.5 V, with a step size of 0.1 V/s.
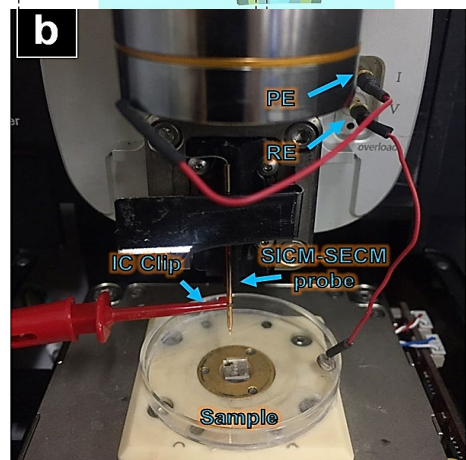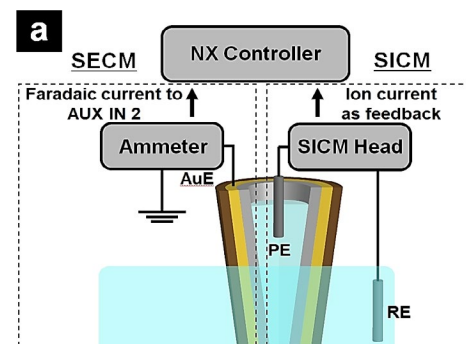
Fig. 6 a) Cartoon illustration of SICM-SECM imaging; b) Setup of the SICM-SECM measurement performed with the probe mounted on the SICM head of a Park NX12 AFM system.

SICM-SECM Imaging

To realize SICM-SECM imaging, a Park NX12 system in combination with an ammeter (Chem Clamp, Dagan Corporation, Minneapolis, MN) is used. A schematic diagram of the SICM-SECM setup is depicted in Figure 6a. Ion current between the Ag/AgCl electrodes inside the pipette (PE: pipette electrode) and another Ag/AgCl pallet electrode in the bath solution (RE: reference electrode) is employed as feedback to control probe-substrate distance.
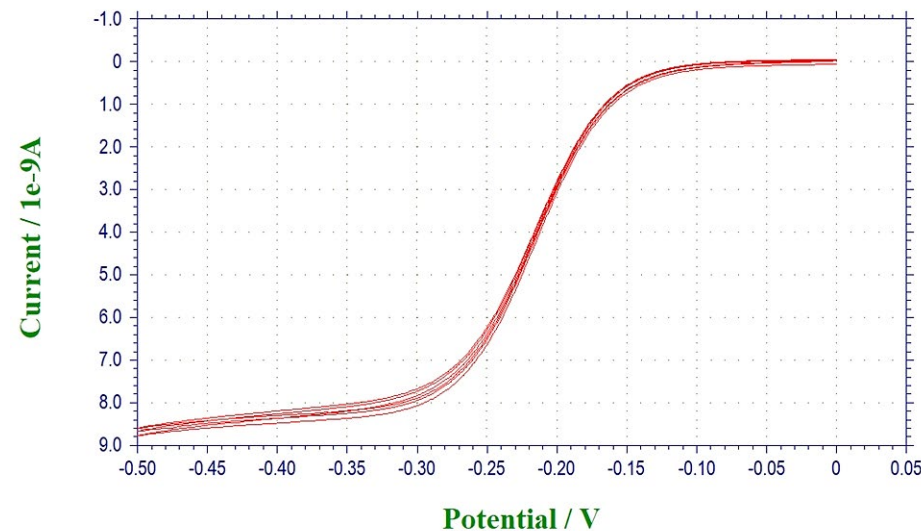
Fig. 7 Cyclic voltammograms (CVs) taken with the Au crescent electrode in bulk solution containing 100 mM KCl and 5 mM Ru(NH3)63+.

The Au crescent electrode (AuE) is used to acquire electrochemical signal. The potential applied between the PE and RE was 0.1 V, and the potential at the Au E was held at -0.5 V. The ammeter is used for both applying potential to the AuE and measuring the faradaic current at the AuE. The measured faradaic current is then fed to one of the auxiliary recording channels (AUX IN 2) of the NX12 controller and recorded in real-time via the SmartScan software. As a result, simultaneous topographical imaging (from SICM) and electrochemical activity mapping (from SECM) is accomplished.

Results and Discussion

As shown in Figure 7, five consecutive CVs taken with the Au crescent electrode in a bulk solution containing 100 mM KCl + 10 mM Ru(NH3)63+ are shown. For Ru(NH3)63+ , starting from ~0.25 V, the reduction reaction of Ru(NH3)63+ to Ru(NH3)62+ takes places, and as the potential is ramped up, at ~-0.5 V, the electrochemical reaction is diffusion-controlled and a steady-state current is reached. The electrochemical reaction is shown below:

$$Ru(NH_3)^{3/}_6{}^+ + e^- \leftrightarrow Ru(NH_3)^{2}_6{}^+$$
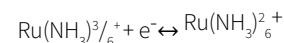
From the CV data, a steady-state current was reached at -0.5 V, and, thus, in the following SICM-SECM imaging experiment, the bias applied to the Au electrode will be kept at -0.5 V.

Height (50μm×25 μm)

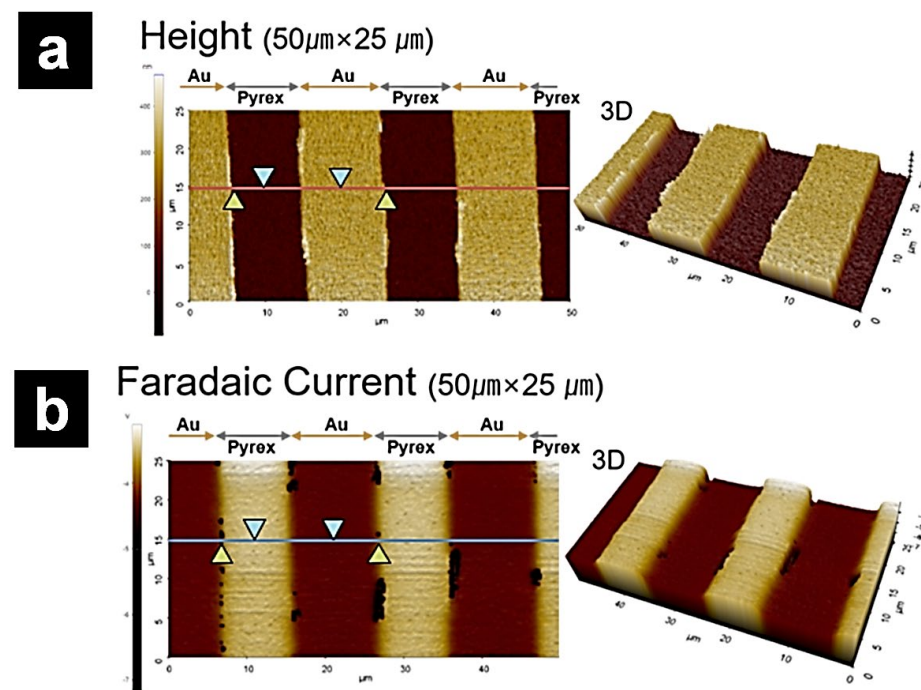### Faradaic Current (50μm×25 μm)

Fig. 8 Representative SICM-SECM images. a) SICM topography image; b) SECM faradaic current image.
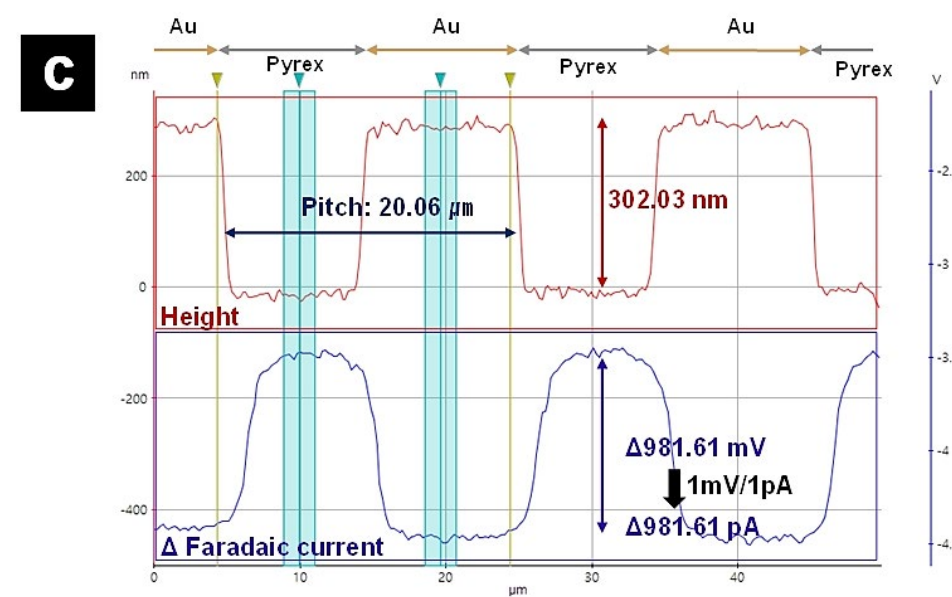
Fig. 8 c) Line profile along the line seen in a) and b). Image size: 50 μm × 25 μm.

In Figure 8, representative SICM-SECM images are shown. In Figure 8a, topography image of the Au/Pyrex pattern is shown. Figure 8c (top) shows the line profile of the topography image. The measured pitch width is 20.06 μm, which matches the actual pitch width (20 μm). The measured height of the Au bar is 302.03 nm, which is, again, agrees with the actual feature height of 300 nm. In Figure 8b, electrochemical activity map of the same region seen in Figure 8a is shown. The absolute value of the faradaic current over Au is ~4.5 nA, while over Pyrex, the absolute value of the faradaic current is ~3.6 nA. An overall ~981 pA faradaic current difference is observed. Correlation of the topography and faradaic current images reveals the expected contrast, with enhanced faradaic current over the conductive Au regions, consistent with positive feedback due to redox cycling, and reduced Faradaic current over insulative Pyrex trenches, consistent with negative feedback due to In Figure 8, representative SICM-SECM images are shown. In Figure 8a, topography image of the Au/Pyrex pattern is shown. Figure 8c (top) shows the line profile of the topography image. The measured pitch width is 20.06 μm, which matches the actual pitch width (20 μm). The measured height of the Au bar is 302.03 nm, which is, again, agrees with the actual feature height of 300 nm. In Figure 8b, electrochemical activity map of the same region seen in Figure 8a is shown. The absolute value of the faradaic current over Au is ~4.5 nA, while over Pyrex, the absolute value of the faradaic current is ~3.6 nA. An overall ~981 pA faradaic current difference is observed. Correlation of the topography and faradaic current images reveals the expected contrast, with enhanced faradaic current over the conductive Au regions, consistent with positive feedback due to redox cycling, and reduced Faradaic current over insulative Pyrex trenches, consistent with negative feedback due to hindered diffusion.

Conclusions

In this application note, we demonstrated the use of a Park NX12 AFM in combination with an ammeter for concurrent topography imaging and electrochemical mapping. The SICM-SECM probe utilized here consisted of a Au crescent electrode (AuE) on the peripheral of a nanopipette. High resolution probe-substrate distance control was obtained by the ion current feedback from SICM, while simultaneous electrochemical signal collection was achieved via the AuE from SECM. As a proof-of-concept experiment, a Au/Pyrex pattern standard sample was imaged with the SICM-SECM technique. The Au bar and the Pyrex substrate were clearly resolved from the SICM topography image, with the bar height and pitch width closely matching the actual values. In terms of the electrochemical property mapping, higher faradaic current was seen when the probe was scanned 0over Au bar as a result of redox cycling, while lower faradaic current was observed when the probe was over Pyrex substrate due to hindered diffusion. The capability of the SICM-SECM technique described here holds promise of many exciting applications in the field of electrochemistry, material science and battery research.

References

[1] Binnig, G., Rohrer, H., Gerber, C. and Weibel, E., Tunneling through a controllable vacuum gap. Appl. Phys. Lett., 1982, 40, 178-180.
[2] Snowden, M. E., Güell, A. G., Lai, S. C., McKelvey, K., Ebejer, N., O'Connell, M. A., Colburn, A. W. and Unwin, P. R. Scanning electrochemical cell microscopy: Theory and experiment for quantitative high resolution spatially-resolved voltammetry and simultaneous ion-conductance measurements. Anal. Chem., 2012, 84, 2483-2491.
[3] Hansma, P. K., Drake, B., Marti, O., Gould, S. A. C. and Prater, C. B. The scanning ion-conductance microscope. Science, 1989, 243, 641.
[4] Chen, C. C., Derylo, M. A. and Baker, L. A. Measurement of ion currents through porous membranes with scanning ion conductance microscopy. Anal. Chem., 2009, 81, 4742-4751.
[5] Korchev, Y. E., Bashford, C. L., Milovanovic, M., Vodyanoy, I. and Lab, M. J. Scanning ion conductance microscopy of living cells. Biophys. J., 1997, 73, 653-658.
[6] Shevchuk, A. I., Gorelik, J., Harding, S. E., Lab, M. J., Klenerman, D. and Korchev, Y. E. Simultaneous measurement of Ca 2+ and cellular dynamics: combined scanning ion conductance and optical microscopy to study contracting cardiac myocytes. Biophys. J., 2001, 81, 1759-1764.
[7] Gorelik, J., Shevchuk, A. I., Frolenkov, G. I., Diakonov, I. A., Kros, C. J., Richardson, G. P., Edwards, C.R., Klenerman, D. and Korchev, Y. E. Dynamic assembly of surface structures in living cells. Proc. Natl. Acad. Sci. U.S.A., 2003, 100, 5819-5822.
[8] Pellegrino, M., Orsini, P. and De Gregorio, F. Use of scanning ion conductance microscopy to guide and redirect neuronal growth cones. Neurosci. Res., 2009, 64, 290-296.
[9] Böcker, M., Muschter, S., Schmitt, E. K., Steinem, C. and Schäffer, T. E. Imaging and patterning of pore-suspending membranes with scanning ion conductance microscopy. Langmuir, 2009, 25, 3022-3028.
[10] Korchev, Y. E., Raval, M., Lab, M. J., Gorelik, J., Edwards, C. R., Rayment, T. and Klenerman, D. Hybrid scanning ion conductance and scanning near-field optical microscopy for the study of living cells. Biophys. J., 2000, 78, 2675-2679.
[11] Gorelik, J., Gu, Y., Spohr, H.A., Shevchuk, A.I., Lab, M.J., Harding, S.E., Edwards, C.R., Whitaker, M., Moss, G.W., Benton, D.C. and Sánchez, D., Ion channels in small cells and subcellular structures can be studied with a smart patch-clamp system. Biophys. J., 2002, 83, 3296-3303.
[12] Shi, W., Zeng, Y., Zhou, L., Xiao, Y., Cummins, T.R. and Baker, L.A., Membrane patches as ion channel probes for scanning ion conductance microscopy. Faraday discussions, 2016, 193, 81-97.
[13] Holt, K.B., Bard, A.J., Show, Y. and Swain, G.M., Scanning electrochemical microscopy and conductive probe atomic force microscopy studies of hydrogen-terminated boron-doped diamond electrodes with different doping levels. J. Phys. Chem. B, 2004, 108, 15117-15127.
[14] Shao, Y. and Mirkin, M.V., Probing ion transfer at the liquid/liquid interface by scanning electrochemical microscopy (SECM). J. Phys. Chem. B, 1998, 102, 9915-9921.
[15] Yamada, H., Ogata, M. and Koike, T., Scanning Electrochemical Microscope Observation of Defects in a Hexadecanethiol Monolayer on Gold with Shear Force-Based Tip – Substrate Positioning. Langmuir, 2006, 22, 7923-7927.
[16] Uitto, O.D. and White, H.S., Scanning electrochemical microscopy of membrane transport in the reverse imaging mode. Anal. Chem., 2001, 73, 533-539.
[17] Wilburn, J.P., Wright, D.W. and Cliffel, D.E., Imaging of voltage-gated alamethicin pores in a reconstituted bilayer lipid membrane via scanning electrochemical microscopy. Analyst, 2006, 131, 311-316.
[18] Shi, W. and Baker, L.A., Imaging heterogeneity and transport of degraded Nafion membranes. RSC Adv., 2015, 5, 99284-99290.
[19] Bard, A.J., Li, X. and Zhan, W., Chemically imaging living cells by scanning electrochemical microscopy. Biosens. Bioelectron., 2006, 22, 461-472.
[20] Bauermann, L.P., Schuhmann, W. and Schulte, A., An advanced biological scanning electrochemical microscope (Bio-SECM) for studying individual living cells. Phys. Chem. Chem. Phys., 2004, 6, 4003-4008.
[21] Adams, K.L., Puchades, M. and Ewing, A.G., In vitro electrochemistry of biological systems. Annu. Rev. Anal. Chem., 2008, 1, 329-355.
[22] Amemiya, S., Guo, J., Xiong, H. and Gross, D.A., Biological applications of scanning electrochemical microscopy: chemical imaging of single living cells and beyond. Anal. Bioanal. Chem., 2006, 386, 458-471.
[23] Edwards, M.A., Martin, S., Whitworth, A.L., Macpherson, J.V. and Unwin, P.R., Scanning electrochemical microscopy: principles and applications to biophysical systems. Physio. Meas., 2006, 27, R63.
[24] Walsh, D.A., Fernandez, J.L., Mauzeroll, J. and Bard, A.J., Scanning electrochemical microscopy. 55. Fabrication and characterization of micropipet probes. Anal. Chem., 2005, 77, 5182-5188.
[25] Comstock, D.J., Elam, J.W., Pellin, M.J. and Hersam, M.C., Integrated ultramicroelectrode– nanopipet probe for concurrent scanning electrochemical microscopy and scanning ion conductance microscopy. Anal. Chem., 2010, 82, 1270-1276.
[26] Takahashi, Y., Shevchuk, A.I., Novak, P., Zhang, Y., Ebejer, N., Macpherson, J.V., Unwin, P.R., Pollard, A.J., Roy, D., Clifford, C.A. and Shiku, H., Multifunctional nanoprobes for nanoscale chemical imaging and localized chemical delivery at surfaces and interfaces. Angew. Chem. Int. Ed., 2011, 50, 9638-9642.

HIGH ENERGY SEARCHES FOR DARK MATTER USING THE LARGE AREA TELESCOPE ON THE FERMI GAMMA-RAY SPACE OBSERVATORY AT STANFORD

AN INTERVIEW WITH DR. ELLIOTT D. BLOOM - PROFESSOR OF PARTICLE PHYSICS AND ASTROPHYSICS, EMERITUS STANFORD

DR. ELLIOTT BLOOM

Group Leader for Stanford Linear Accelerator Center (SLAC)

Group K - Dr. Bloom studies Particle Astrophysics with emphasis on the measurement of phenomena associated with regions of high field gravity. Such phenomena are associated with neutron star and black hole candidate systems. His work includes space based X-Ray timing and high energy gamma-ray telescopes offer a powerful tool to experimentally probe such objects including current observations with the USA x-ray telescope, and design and construction of the Large Area Gamma-ray Space telescope.

Group K is located at the Stanford Linear Accelerator Center, a part of Stanford University. The major research interests of Group K are in particle astrophysics. This exciting new discipline merges the worlds of particle physics and astrophysics to try to address some of the most fundamental questions about our universe. Particle astrophysicists use high-energy observations of super-massive black holes and other types of cosmic objects in order to: Test the standard model of particle physics under extreme conditions of temperature, density and magnetic field that cannot be reproduced in

laboratories; Discover possible new types of elementary particles using powerful astrophysical sources; Test the nature of relativistic gravity in environments which have extreme gravitational fields; and Probe the universe on very short and very long timescales using space-based experiments which detect X- and gamma-radiation.

The Fermi-LAT community has been collecting information about the Universe for 10 years.

Fermi is a powerful gamma ray space observatory that has opened a wide window on the universe. Gamma rays are the highest-energy form of light, and the gamma-ray sky is spectacularly different from the one we perceive with our own eyes. With a huge leap in all key capabilities, Fermi data is enabling scientists to answer persistent questions across a broad range of topics, including super massive black-hole systems, pulsars, the origin of cosmic rays, and searches for signals of new physics. The mission is an astrophysics and particle physics partnership, developed by NASA in collaboration with the U.S. Department

of Energy, along with important contributions from academic institutions and partners in France, Germany, Italy, Japan, Sweden, and the United States. Fermi (formerly known as Gamma-ray Large Area Space Telescope, or GLAST) was launched on June 11, 2008. It is named after Enrich Fermi, an Italian-American scientist who did pioneering work in high-energy physics.

Theories of dark matter, mainly invented by Particle Physicists, propose that it is a new sector of matter very different than normal matter

In 1992 a group of physicists at Stanford came up with an idea. They wanted to develop a large telescope to see the entire universe and the gamma ray sky in order to find out more about dark matter. To this day, particle physicists don't agree on what dark matter is, yet it makes up as much as 90% of matter. With this new Gamma Ray Telescope, the largest ever launched in space, this group of physicists wanted to find out more about dark matter and the hi energy universe we cannot see.

After winning an announcement of opportunity from NASA, the GLAST collaboration began, gathering funding from an international team including United States, NASA, DOE and Sweden, Italy, Japan, Germany, & France. Construction took place at the University of CA Santa Cruz and the GLAST (renamed FERMI Gamma Ray Telescope) was launched in 2008.

Now after ten years in space, the scientists have some results. And they have done way beyond what they initially thought they could do.

Viewing 12 billion Years of Starlight with FERMI LAT

The predecessor, EGRET could only view 1,000 sources where the Fermi LAT could record 10,000, thereby viewing a much larger area. In fact, in just one week, orbiting around the Earth every 90 minutes, the FERMI LAT collected more data on gamma rays than all the other studies combined. To put it into perspective, the FERMI LAT can see up to 12 billion light years away, since the formation of the universe began.

Particle Physicists have detected 17 particles and 4 forces, but what FERMI LAT tells us is that there are possibly other particles we haven't identified and other forces acting on them. From Astro physical energy sources, the SLAC's linear accelerator cosmic version of hi energy charged particles depict an extremely violent universe. Only 5% of the universe is described by the standard module of particle physics.

"There are a number of ways to look for experimental signatures of dark matter (beside gravitational signatures that is the reason we believe dark matter exists). The Fermi-LAT telescope uses "indirect detection" techniques and another method uses "direct detection". There is a third method that is exemplified by searches for dark matter at the Large Hadron Collider (LHC) at the CERN lab in Switzerland. The LCH searches for dark matter by attempting to produce it using its high energy circulating beams of protons in proton-proton collisions. Except for indications from gravitational interactions, all of these techniques have so far come up empty with no observation of dark matter, just limits. Currently, theory indicates that we should be searching using all three experimental techniques as one or the other may be more sensitive, though unpredictably so." Dr. Elliott Bloom, Professor of Particle Physics and Astrophysics, Emeritus Stanford

Dark Matter, the Invisible Component. The one that does not emit light remains for the most part a mystery, but FERMI LAT can tell you a lot about it.

The largest all sky telescope, Fermi has answered persistent questions about super massive black-hole systems, pulsars, the origin of cosmic rays, and searches for signals of new physics. Dr. Eric Charles who has been on the project since 2005, three years before it launched said that he came to the project because it was a new kind of telescope and incredibly appealing.

Our eyes have evolved to create a view that makes sense, but there is so much more to see. In his recent talk at SLAC "10 Years of Cosmic Fireworks with FERMI", he presents five of the highlights of the mission ranging from terrestrial gamma ray flashes and from the sun to measuring all the starlight in the universe.

The LAT collaboration includes more than 400 scientists and students at more than 90 universities and laboratories in 12 countries.

Above is a picture of some Fermi-LAT Collaboration members who gathered at the SLAC National Accelerator Laboratory on the 10th anniversary of the Fermi Gamma-ray Space Telescope (FGST) on June 11, 2018. There are about 400 members of the Fermi-LAT Collaboration worldwide. The group of 37 in the picture is mainly (but not all) from SLAC/Stanford University, and includes scientists and engineers that helped design and build the Fermi-LAT, maintain its operations in space, and analyze the data transmitted from the space telescope by NASA to SLAC. Above the group hangs a ½ scale model of the Fermi-LAT. Dr. Elliott Bloom pictured 2nd row in red shirt. Credit: SLAC National Accelerator Laboratory Communications Department

Gamma Rays are electromagnetic short wave lengths with lots of energy at a very high frequency, 1/billionth of an atom at 2 trillion degrees Celsius. Gamma Rays which have billion electron volts are formed by the accelerating hi energy charged particles and are visible with the FERMI LAT.

The hi energy universe was dramatically influenced by FERMI in the last 10 years, thru FERMI we have learned a lot about pulsars, states Dr. Bloom

Pulsars are rapidly spinning neutron stars, super dense objects forged when a massive star collapses and explodes as a supernova. Young neutron stars spin dozens of times a second and gradually slow with age. But if an aging pulsar is paired with a normal star in a binary system, their interaction may ramp up the neutron star's spin to hundreds of rotations each second, creating what astronomers call a millisecond pulsar. Dizzying spin coupled with super strong magnetic and electric fields make pulsars superb natural particle accelerators, nearly 1,000 times more powerful than any machine on Earth. Originally discovered nearly 50 years ago by their radio emissions, more than 2,000 pulsars have been identified to date. Radio telescopes - and later, satellites with detectors sensitive to X-rays and gamma rays - detect a quick pulse whenever a pulsar's

rotation sweeps its beam of emission across our field of view.

With a big budget increase for particle physics this year (800 million), future scientists searching for answers to the mysterious dark matter can go back to fundamental science says Dr. Bloom. Applied science was doing very well, he says, but science was dying. Fundamental science is the long term. "Since we don't know what dark matter is, and it does look like some kind of matter - that's the excitement of science."

Some Fermi-LAT Collaboration members gathered at the SLAC National Accelerator Laboratory on the 10th anniversary of the Fermi Gamma-ray Space Telescope (FGST) on June 11, 2018

The LAT collaboration includes more than 400 scientists and students at more than 90 universities and laboratories in 12 countries.
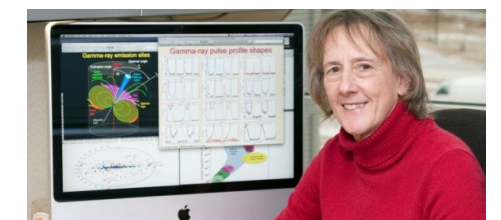
Above: Alice Harding studies how gamma-ray pulsars work using observations from NASA's Fermi Gamma-Ray Space Telescope
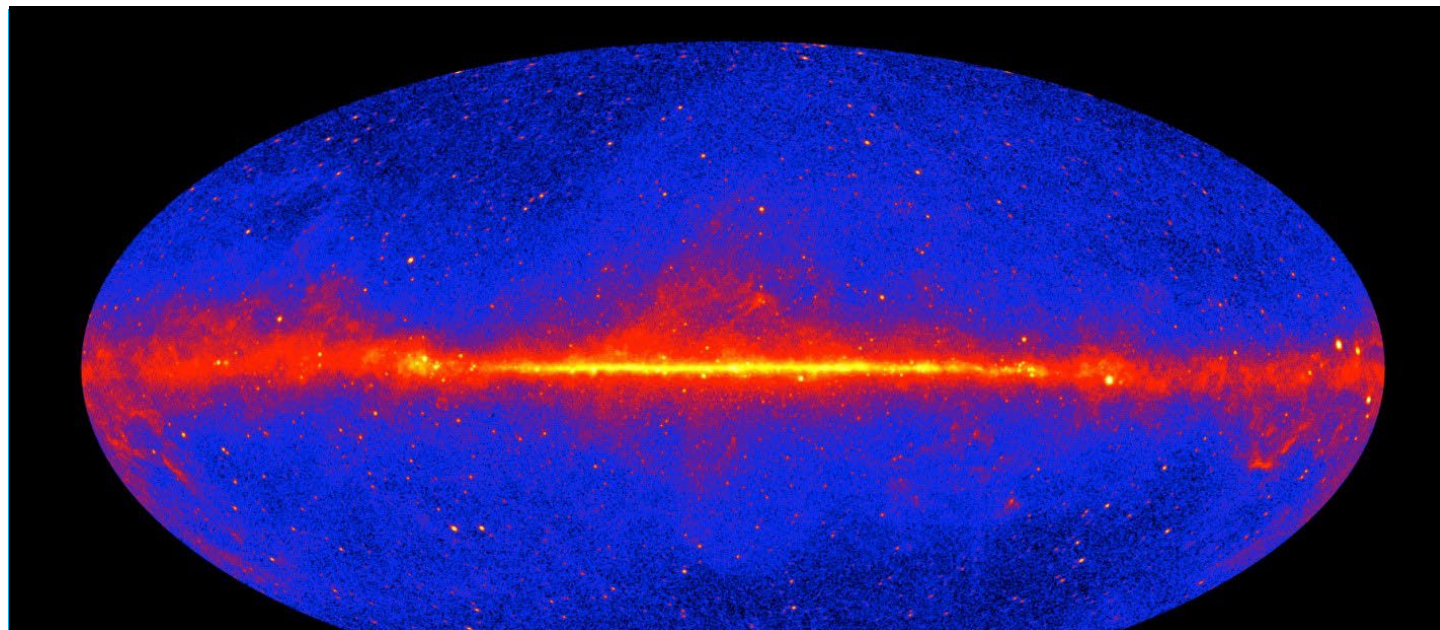
ALL SKY INTENSITY MAP DERIVED FROM 9 YEARS OF FERMI-LAT DATA SHOWS THE ENTIRE UNIVERSE

This picture is an all sky intensity map derived from 9 years of Fermi-LAT data, (August 4, 2008 - August 4, 2017) time integrated all-sky image (based on Pass 8 Source class, PSF3 event type-internal collaboration notation). The map is also integrated above 1 GeV (that is 1 billion electron volt energy gamma rays and above up to about 1 trillion electron volt energy). The intensity scale is false color with low intensity black and high intensity white. The map shows the entire universe in standard astronomical Galactic coordinates (in what is called a Hammer-Aitoff projection – not simple), these coordinates and projection have the center of our galaxy at the center of the picture (very bright), and the anticenter of the galaxy at the edges of the picture centerline (the anticenter is in the direction out from the Galactic center along the Galactic center-sun axis) The images are smoothed with a 0.25 deg FWHM Gaussian. The maps are in intensity units. The images have a logarithmic scaling, from about 3 x 10-7 gamma rays per cm-2 s-1 sr-1 to 1 x 10-3 gamma rays per cm-2 s-1 sr-1. The actual maximum intensity in the map is 0.02 cm-2 s-1 sr-1. (cm-2 is per square centimeter of detector area, s-1 is per sec and sr-1 is per steradian). The images are 3600x1800 (0.1 degree pixels). The bright dots are point sources of gamma rays in the sky, and many of these are

time variable that you don't notice in this time lapse image. The band that you see horizontally across the picture is the Milky Way Galaxy (our galaxy). Above this plane and below this plane are gamma ray sources from the rest of the universe and typically many millions to billions of light years away from us. Not so obvious in this picture are the "Fermi Bubbles" the diffuse structures that protrude above and below the region of the Galactic center. These structures are thought to be remnants of energetic jet activity powered by the central black hole of our galaxy in times long past and were discovered using Fermi-LAT data.
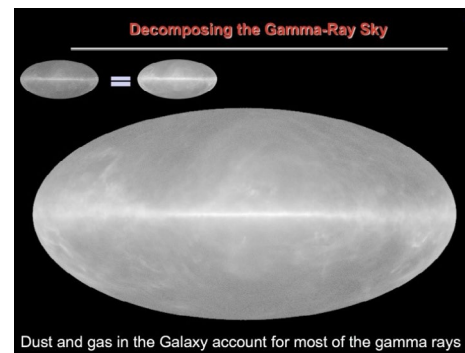
Photo Credit: Fermi-LAT Collaboration

## PICTURE SERIES INDICATING HOW WE DECOMPOSE THE GAMMA RAY SKY

*(Photos and Captions provided by Dr. Elliott Bloom, Fermi-LAT)*
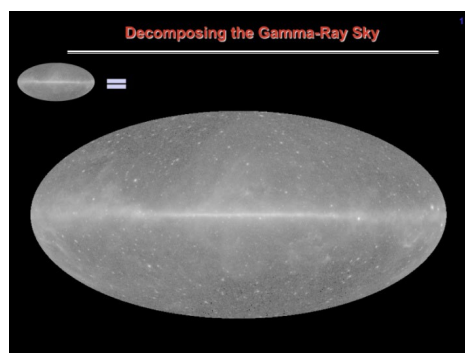
*Picture 1: All-Sky intensity in black and white*

Picture 2: Diffuse - in a complex analysis we can isolate the Galactic diffuse signal and it looks as in this picture. This gamma ray signal mostly originates in the interaction of Galactic cosmic rays with the gas of the Galaxy.
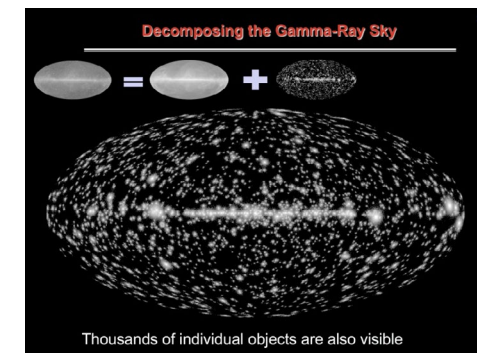
Picture 3: Point sources - In different complex analysis we can extract the point and near point sources of gamma rays.
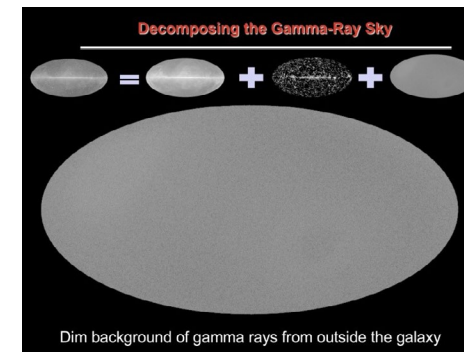
Picture 4: Extra Galactic diffuse – In yet a different complex analysis we can extract the diffuse gamma ray radiation coming from beyond our galaxy, likely from the furthest reaches of the universe. This diffuse is uniform from all directions.
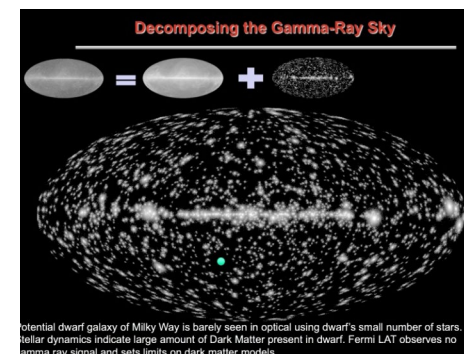

Picture 5: Use Dwarf Galaxies to search for dark matter - This picture is similar to the point sources in which I try to demonstrate how we can set limits on gamma rays coming from dark matter particle decay or annihilation- with another DM particle. There are now about 60 dwarf satellite galaxies of the Milky Way that have been discovered and new ones are discovered every year via ground based optical telescope surveys of the sky. One can measure from the stellar motions in these galaxies using big optical telescopes that they are heavily dark matter dominated.

Looking for Dark Matter by Observing Dwarf Galaxies

Dark matter makes up about 28% of the matter in the universe. Regular matter that we are used to makes up about 5% of the matter in the universe. The rest of the energy density of the universe is made up of dark energy. Thus about 80% of the matter in the universe is of a very different kind than the matter we know about-all of the elements of the periodic table, and does not shine so we can see it in any kind of EM radiation from radio to gamma rays. Theories of dark matter, mainly invented by Particle Physicists, propose that it is a new sector of matter very different than normal matter. What is it?

The Fermi-LAT community has be searching
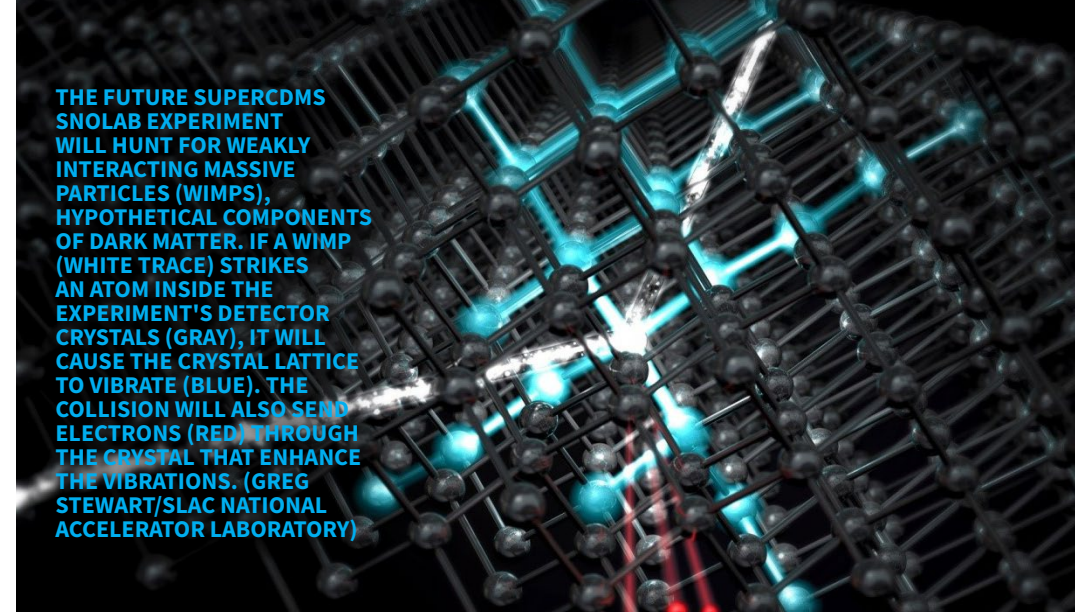
for emission of gamma -rays from dark matter that has been predicted by theoretical models of what might make up the dark matter (new types of elementary particles).

This last picture shows as a green dot a hypothetical dwarf galaxy located where there are no gamma ray point sources (this is typical in our data, though this sky location is hypothetical). Optical telescopes would measure the presence of a small galaxy with not too many stars, and also indicate that the dwarf galaxy was dark matter dominated.

Fermi knows where to look as the optical telescopes precisely establish the location of this dwarf galaxy. When the Fermi – LAT does its observations and analysis of this spot it finds no emission of gamma-rays, and then we can set limits on the gamma ray intensity from this dwarf. These limits challenge theories of particle dark matter that predict the Fermi-LAT should have observed gamma-rays from this source. There are a number of other ways that the Fermi – LAT can search for dark matter gamma ray signals, but using dwarf galaxies has proven so far to give the most stringent limits on dark matter gamma ray emission.

New Search Underway for the Dark Matter at SLAC

Scientists know that visible matter in the universe accounts for only about 15% of all matter and the rest is a mysterious substance, called dark matter. Due to its gravitational pull on regular matter, dark matter is a key driver for the evolution of the universe, affecting the formation of galaxies like the Milky Way. Still searching for what dark matter is made of, scientists at SLAC believe it could be composed of dark matter particles, and WIMPs are top contenders. If these particles exist, they would barely interact with their environment and fly right through regular matter untouched. However, every so often, they could collide with an atom of our visible world, and dark

matter researchers are looking for these rare interactions.

Construction Begins on One of the World's Most Sensitive Dark Matter Experiments

The SuperCDMS SNOLAB project, a multi-institutional effort led by SLAC, is expanding the hunt for dark matter to particles with properties not accessible to any other experiment.

U.S. Department of Energy funded the construction of SuperCDMS SNOLAB experiment, which will begin operations in the early 2020s to hunt for hypothetical dark matter particles called weakly interacting massive particles, or WIMPs. The DOE Office of Science will contribute $19 million to the effort, joining forces with the National Science Foundation ($12 million) and the Canada Foundation for Innovation ($3 million). The DOE's SLAC National Accelerator Laboratory is managing the construction project for the international SuperCDMS collaboration of 111 members from 26 institutions, which is preparing to do research with the experiment.

The experiment will be at least 50 times more sensitive than its predecessor, exploring WIMP properties that can't be probed by other experiments and giving researchers a powerful new tool to understand one of the biggest mysteries of modern physics, what is dark matter?

"Understanding dark matter is one of the hottest research topics – at SLAC and around the world," said JoAnne Hewett, head of SLAC's Fundamental Physics Directorate and the lab's chief research officer. "We're excited to lead the project and work with our partners to build this next-generation dark matter experiment." For more information go to: https://www6.slac.stanford.edu/news/2018-05-07-construction-begins-one-worlds-most-sensitive-dark-matter-experiments.aspx